Modeling for spectroscopic diagnostics of CCP-ICP and PBIF plasmas in KAERI

Duck-Hee Kwon, Changmin Shin, Haewon Shin

and Kil-Byoung Chai

2023. 7. 12

KAERI Korea Atomic Energy Research Institute

Nuclear Data Center
Nuclear Physics Application Research Division

E-mail: hkwon@kaeri.re.kr, kbchai@kaeri.re.kr
https://pearl.kaeri.re.kr

Contents

- Collisional-radiative modeling (CRM) for He, H/D plasmas
  - Modeling methods and AM data
  - Sensitivities to used AM data and plasma parameters

- S/XB ratio for sputtering yield of W
  - S/XB ratio methods and atomic data
  - Experimental S/XB ratios

Contents

- Collisional-radiative modeling (CRM) for He, H/D plasmas
  - Modeling methods and AM data
  - Sensitivities to used AM data and plasma parameters

- S/XB ratio for sputtering yield of W
  - S/XB ratio methods and atomic data
  - Experimental S/XB ratios

OES in low temperature plasmas

Experimental setup

CCP: Capacitively Coupled Plasma
ICP: Inductively Coupled Plasms

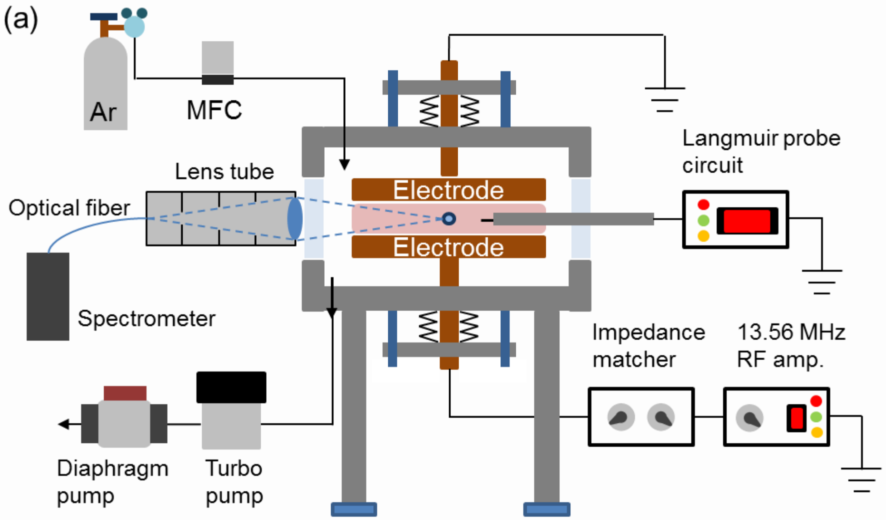

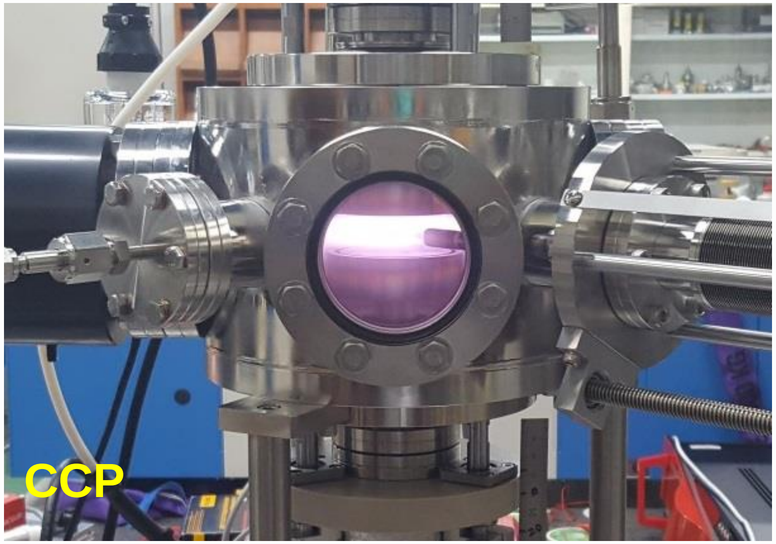

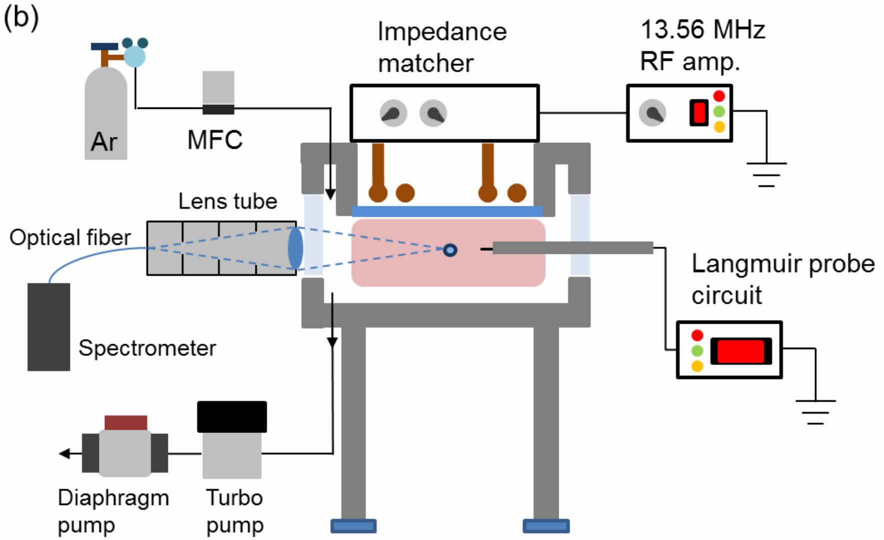

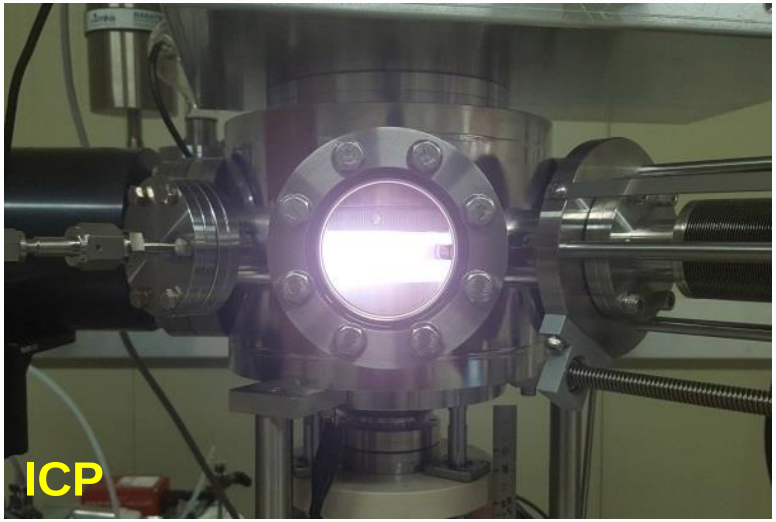

CRM for low temperature He I plasma

Steady state balance equation for excited levels

From the particle balance equation $\frac{\partial n}{\partial t} + \nabla \cdot (n\mathbf{u}) = \frac{\delta n}{\delta t}$, $n\mathbf{u} = -\nabla(D_a n)$

$$\frac{\partial N_i}{\partial t} - \nabla \cdot (\nabla D_a N_i) = \left(\frac{\delta N_i}{\delta t}\right)_{CR},\ \nabla \cdot (\nabla D_a N_i) \approx \nu_i^d N_i\ ,\ \frac{\partial N_i}{\partial t} = 0$$

In the weakly ionizing plasma conditions $N_0 \alpha_I \gg n_+ \alpha_R$, $n_+ \approx n_e$

Populating terms **Depopulating terms**

$$\sum_{j \neq i} n_e \alpha_{ji}^{ex} N_j + \sum_{j>i} \eta_{ji}(N_i) A_{ji} N_j = \sum_{j \neq i} n_e \alpha_{ij}^{ex} N_i + \sum_{j<i} \eta_{ij}(N_j) A_{ij} N_i + n_e \alpha_i^{\mathrm{I}} N_i + \sum_j \alpha_{ij}^{\mathrm{I}} N_i N_j + \nu_i^d N_i$$

Nonlinear terms

Ground level population

$$p_{tot} = N_0 k_B T_g + n_+ k_B T_i + n_e k_B T_e \approx N_0 k_B T_g$$

$$N_0 \cong \frac{p_{tot}}{k_B T_g}\ (constant)$$

Diagnostics for plasma parameters

Minimization of $\Delta(n_e, T_{eff}, R_{eff}, L_{eff}) = \sum \left(\frac{I_{ik}^{\mathrm{CRM}} - I_{ik}^{\mathrm{OES}}}{I_{ik}^{\mathrm{OES}}}\right)^2$, $\quad I_{ik}^{\mathrm{CRM}} = \frac{N_i \eta_{ik} A_{ik}}{\lambda_{ik}}$

Gas temperature for He I plasma

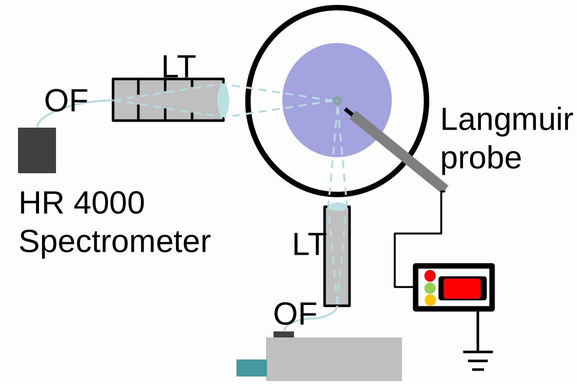

LT: lens tube
OF: optical fiber
MFC: mass flow controller

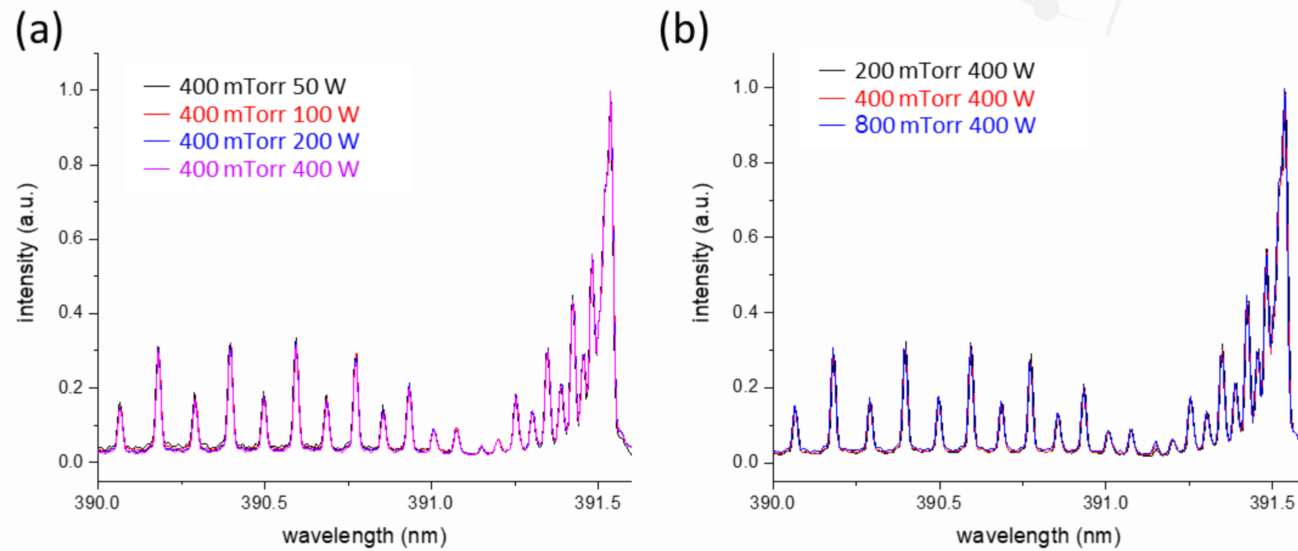

Measured spectra for N_2^+

Gas temperature

T_g can be estimated with the N_2^+ rotational temperature obtained from the emission spectra of the N_2^+ transition $B^2\Sigma_u^+, v = 0 \rightarrow X^2\Sigma_g^+, v' = 0$ by inserting small amount of N_2 gas into the He plasma.

(c)

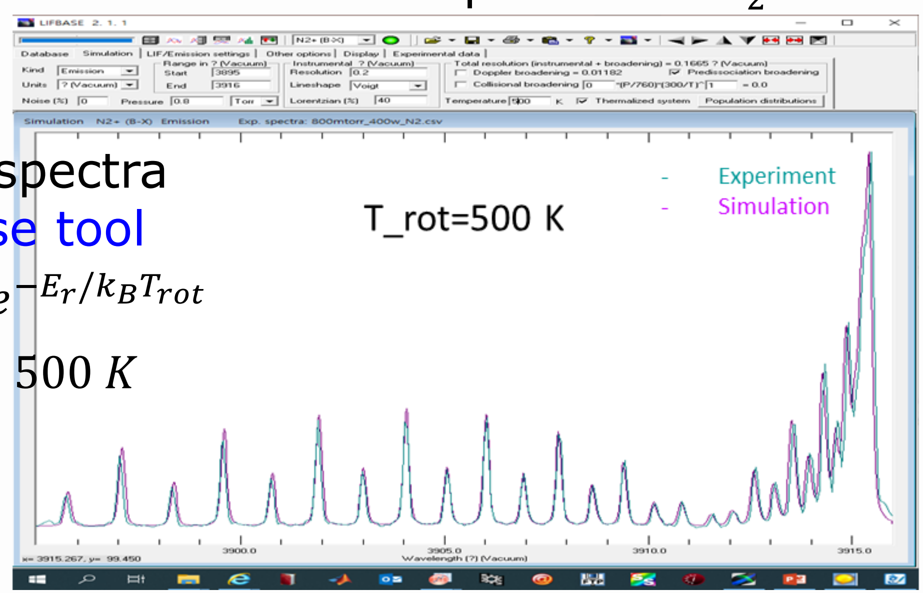

Modeled spectra
by LIFbase tool

$$I = D_0 k^4 S e^{-E_r/k_B T_{rot}}$$

$$\Rightarrow T_g \approx T_{rot} = 500\ K$$

Energy levels and Kinetic processes of He I

Energy levels

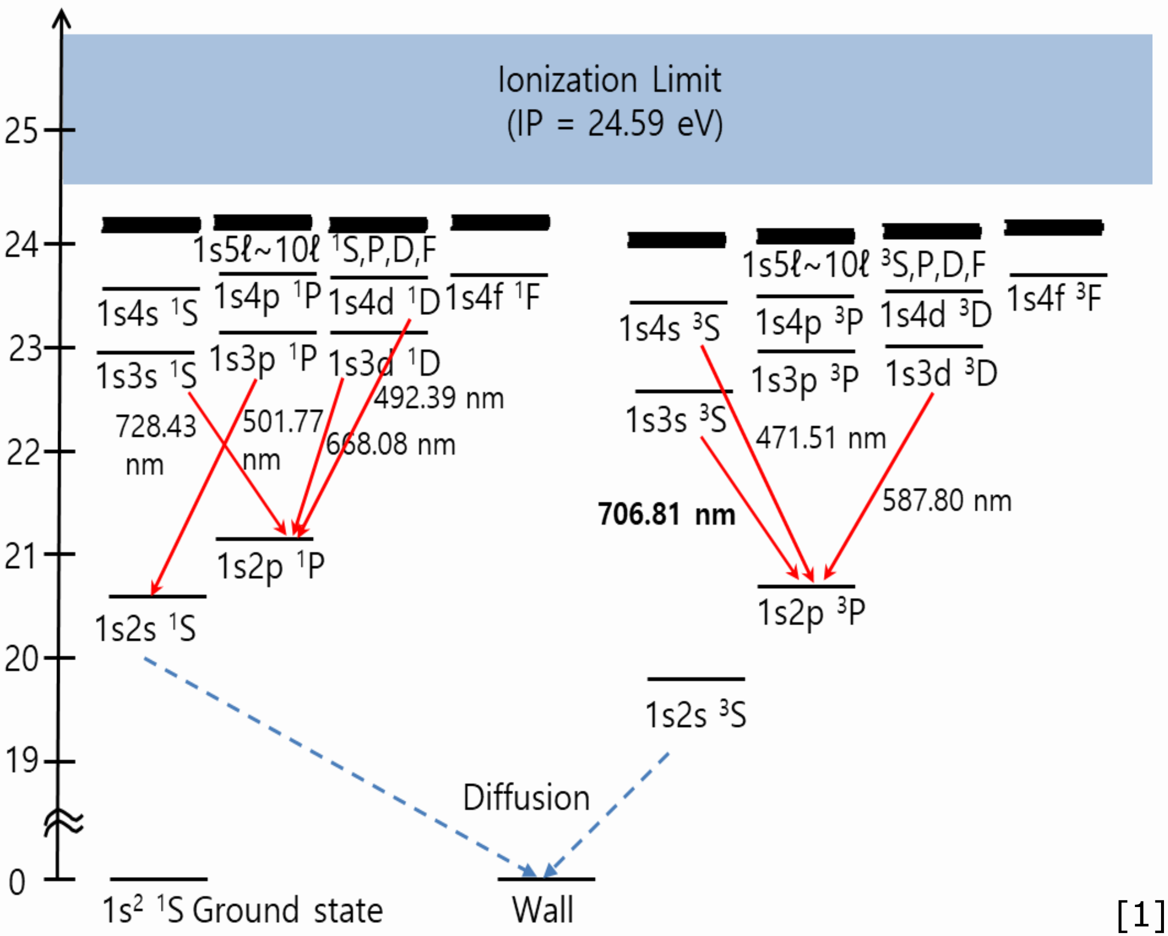

$up\ to\ 1snl\ (n = 10, \ell = 3)$

Kinetic processes

1. $\mathrm{He} + \mathrm{e} \rightarrow \mathrm{He}^{*} + \mathrm{e}$ $\quad \alpha_{ij}^{ex}$ [1]
2. $\mathrm{He} + \mathrm{e} \rightarrow \mathrm{He}^{+} + 2\mathrm{e}$ $\quad \alpha_{i}^{\mathrm{I}}$ [1]
3. $\mathrm{He}^{*} \rightarrow \mathrm{He} + h\nu$ $\quad \lambda_{ij}, A_{ij}$ [2]
4. $\mathrm{He}(1s2\ell) + \mathrm{He}(1s2\ell') \rightarrow \mathrm{He}^{+} + \mathrm{He} + \mathrm{e}$ $\quad \alpha_{ij}^{\mathrm{I}}$

$$2.9 \times 10^{-9}\left(T_g/300\right)^{1/2}(cm^3/s)$$

5. $\mathrm{He}(1s2s) \rightarrow to\ wall$ $\quad \nu_i^d$

$$\nu_i^d = D_a\left(\left(\frac{2.405}{R_{eff}}\right)^2 + \left(\frac{\pi}{L_{eff}}\right)^2\right),$$

$$D_a = 8.992 \times 10^{-2}\,\frac{T_g^{3/2}}{p}\ (cm^3/s)$$

[1] Y. Ralchenko, R. K. Janev, T. Kato, D. V. Fursa, I. Bray, F. J. de Heer, Atomic Data and Nuclear Data Tables 94 (2008) 603.

[2] G.W.F Drake, D.C. Morton, Astrophys. J. Suppl. Series 170 (2007) 251.

Results for diagnostics

Non-Maxwellian electron energy distribution

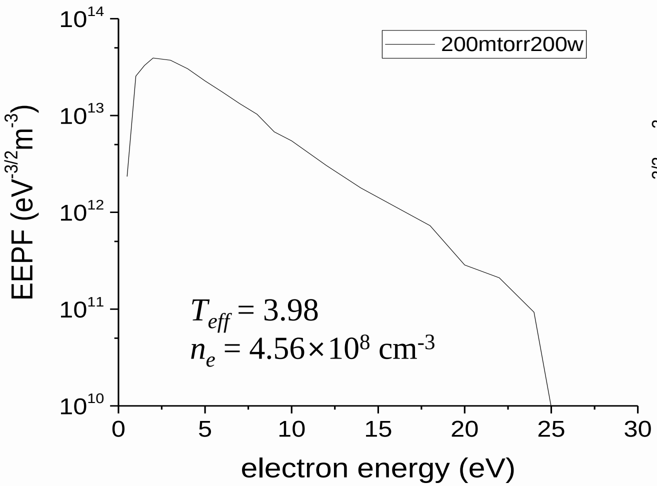

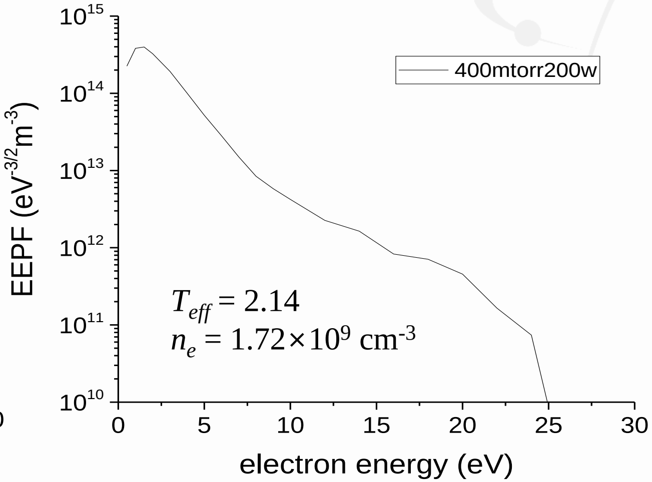

OES and CR modeling spectra

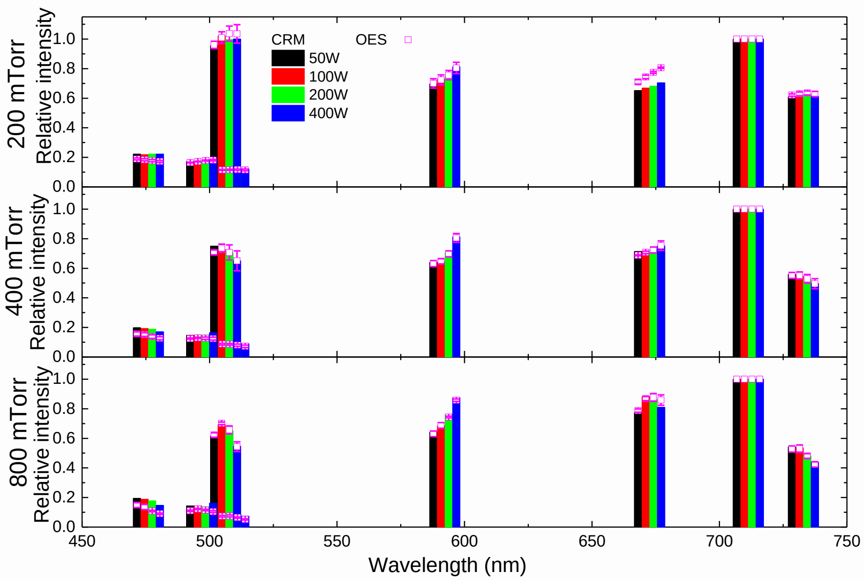

Electron temperature and density

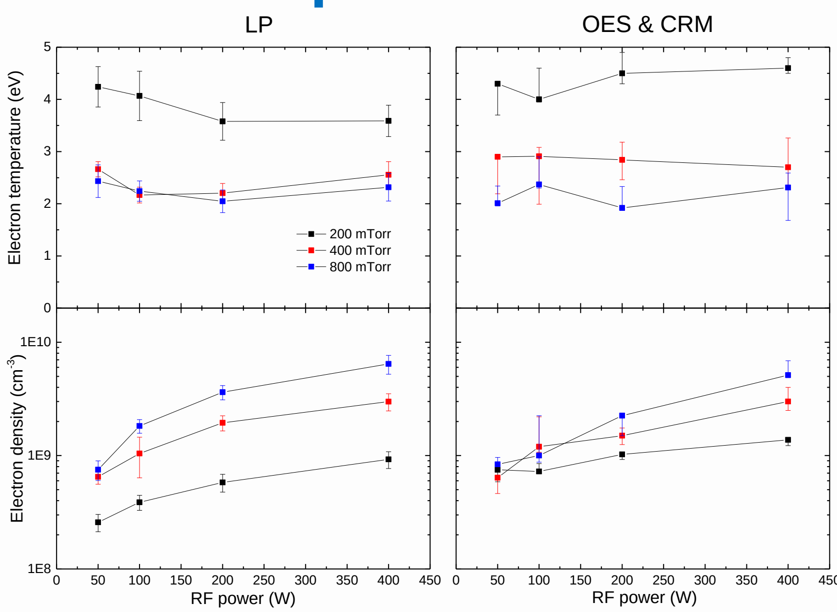

K.-B. Chai and D.-H. Kwon, Spectrochimica Acta Part B **183** 106269 (2021).

Population kinetics for He I

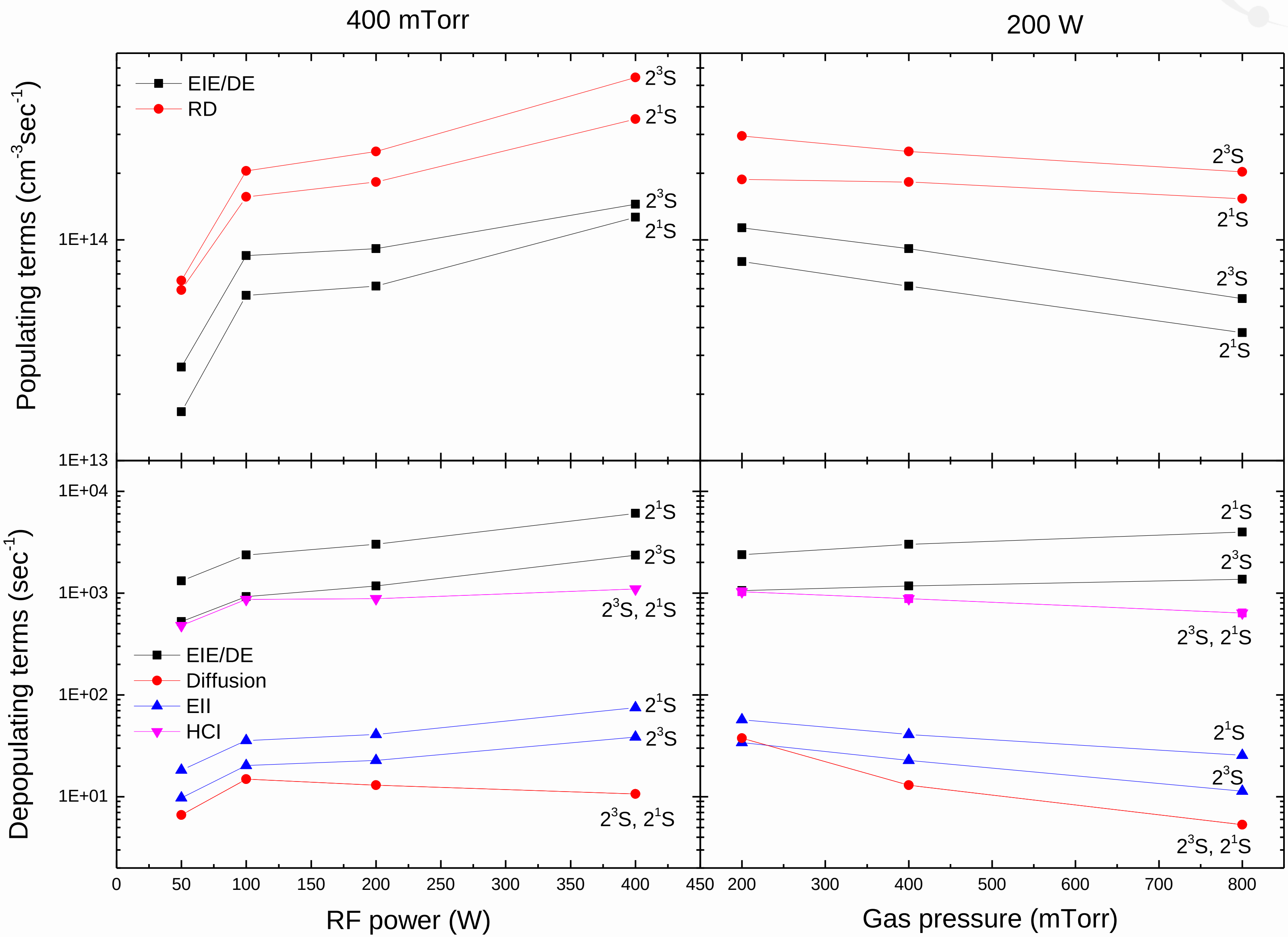

Deviation from Boltzman distributions

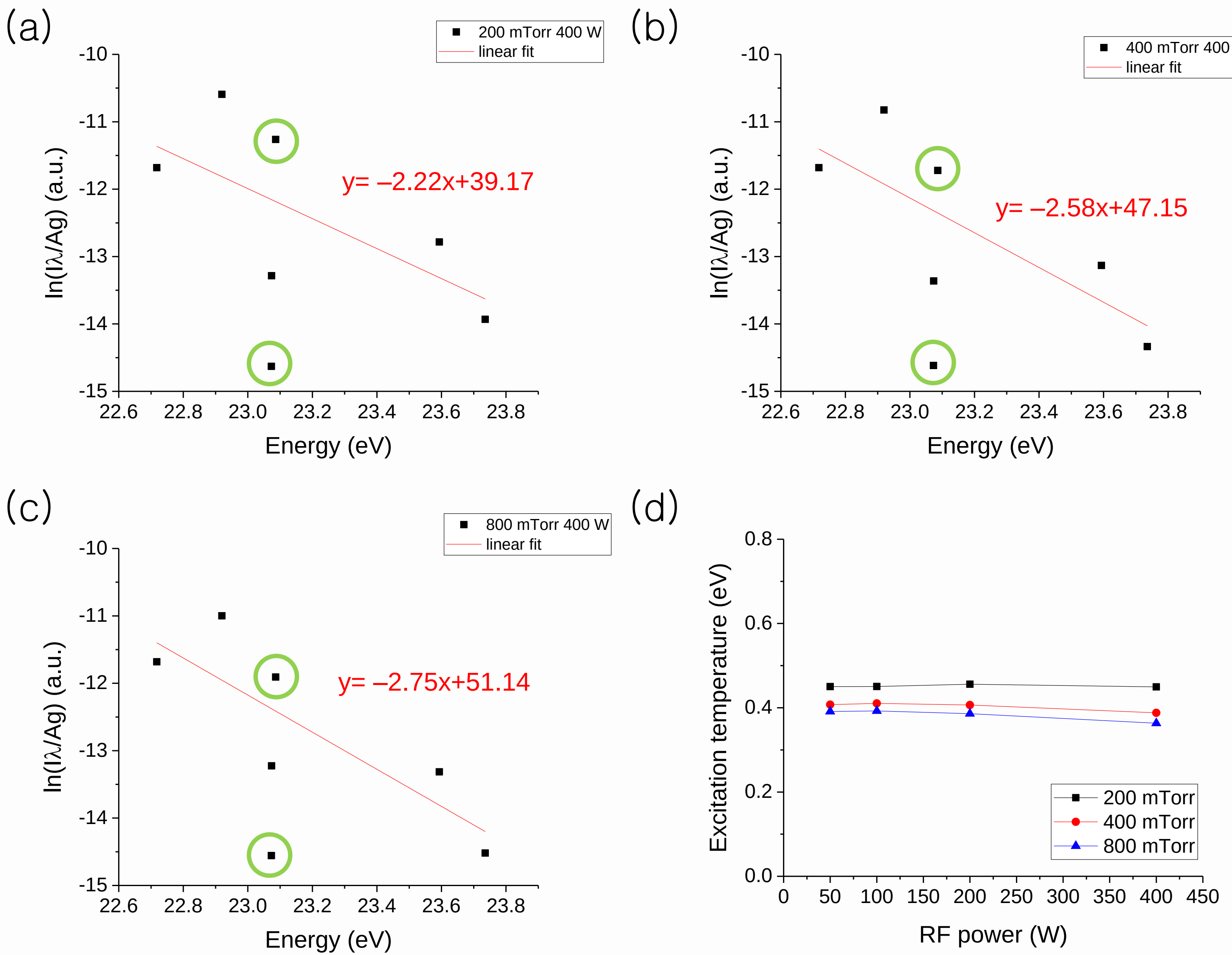

KAERI Plasma Beam Irradiation Facility

Motivation of the construction

In order to develop divertor materials and cooling techniques resisting **high heat** and **particle fluxes** (heat flux of 10 MW/m^2 and particle flux of 10^{24} $/m^2s$ will come in ITER and much larger heat and particle fluxes will come in DEMO), we have constructed **lab-scale** divertor plasma simulator

Applied field-magnetoplasmadynamic (AF-MPD) thruster concept

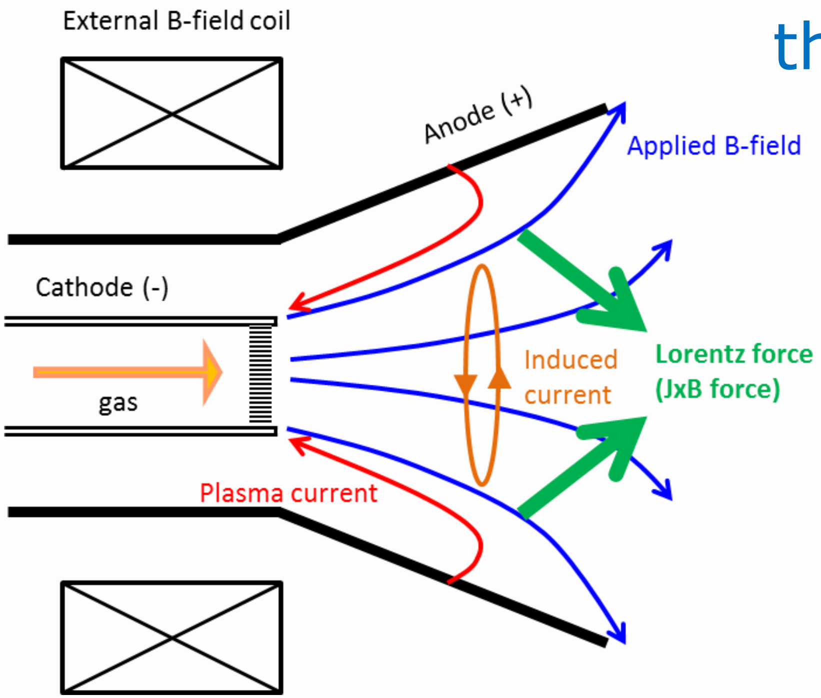

type I/ type II — type I/ type II

- Anode radius = 4/2 cm, cathode radius = 0.6/0.4 cm
- Anode material: Cu, cathode material: W+ThO_2 (2%)
- Insulating material : ceramic (Al_2O_3)
- Sustain power supply : DC 10-20 kW
- External B-field: 0.17 T (NdFeB permanent magnet)
- Both anode & cathode can be water-cooled

KPBIF schemes and measurement

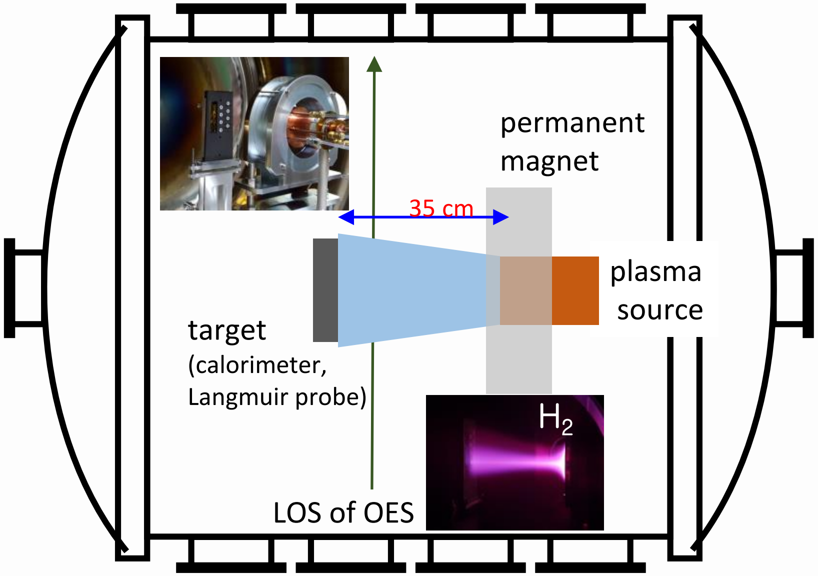

Plasma source schemes

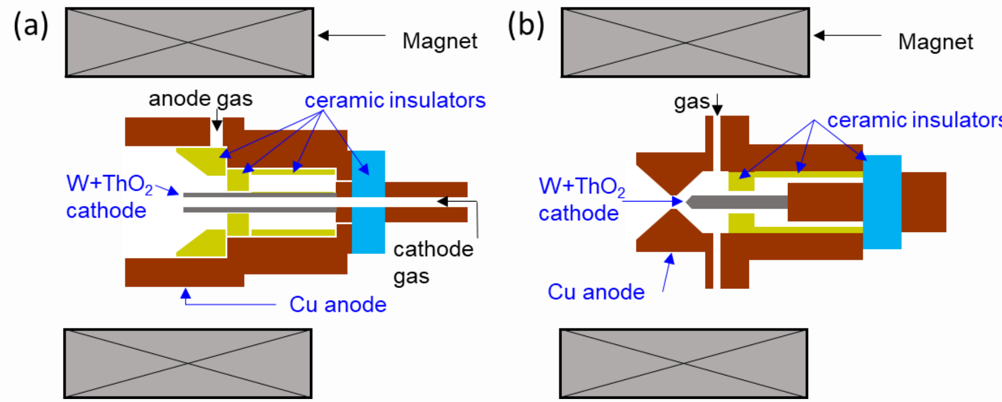

Type I for Ar

Type II for H_2,D_2,He

Electron temperature and density by LP

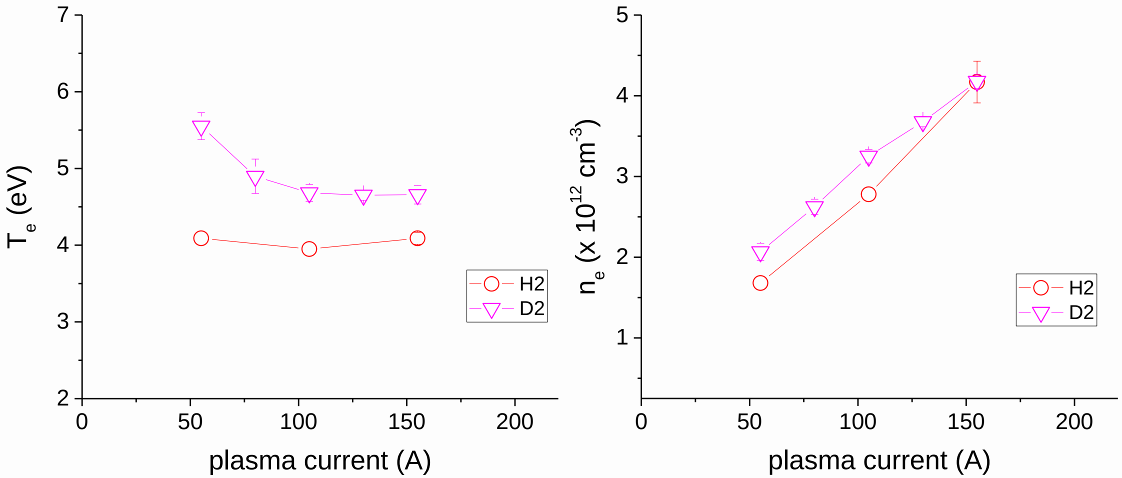

K.-B. Chai, D.-H. Kwon and M. Lee, Plasma Phys. Control. Fusion **63** 125020 (2021)

CRM for H/D plasma

Considered processes

$\mathrm{H}(n \geq 1) + e \leftrightarrow \mathrm{H}(n' > n) + e$	(1)	[1]
$\mathrm{H}(n \geq 1) + e \leftrightarrow \mathrm{H}^+ + 2e$	(2)	[1]
$\mathrm{H}(n \leq 40) \rightarrow \mathrm{H}(n' < n) + h\nu$	(3)	[1]
$\mathrm{H}^+ + e \rightarrow \mathrm{H}(n \leq 40) + h\nu$	(4)	[1]
$\mathrm{H}_2 + e \rightarrow \mathrm{H}(n = 1) + \mathrm{H}(n' \leq 3) + e$	(5)	[2]
$\mathrm{H}_2 + e \rightarrow 2\mathrm{H}(n = 2) + \mathrm{e}$	(6)	[2]
$\mathrm{H}_2 + e \rightarrow \mathrm{H}^+ + \mathrm{H}(n = 1) + e$	(7)	[1]
$\mathrm{H}_2 + e \rightarrow \mathrm{H}_2^+ + 2e$	(8)	[1]
$\mathrm{H}_2^+ + \mathrm{e} \rightarrow \mathrm{H}(n = 1) + \mathrm{H}(n' \geq 2)$	(9)	[3]
$\mathrm{H}_2^+ + \mathrm{e} \rightarrow \mathrm{H}^+ + \mathrm{H}(n \leq 2) + e$	(10)	[3]
$\mathrm{H}_2^+ + \mathrm{e} \rightarrow 2\mathrm{H}^+ + e$	(11)	[3]
$\mathrm{H}_2^+ + \mathrm{e} \rightarrow \mathrm{H}_2^* \rightarrow \mathrm{H}(n = 1) + \mathrm{H}(n' \geq 2)$	(12)	[1]
$\mathrm{H}_3^+ + \mathrm{e} \rightarrow 3\mathrm{H}(n = 1)$	(13)	[3]
$\mathrm{H}_3^+ + \mathrm{e} \rightarrow \mathrm{H}_2 + \mathrm{H}(n = 2)$	(14)	[3]
$\mathrm{H}_3^+ + \mathrm{e} \rightarrow \mathrm{H}^+ + 2\mathrm{H}(n = 1) + e$	(15)	[3]
$\mathrm{H}_2^+ + \mathrm{H}_2 \rightarrow \mathrm{H}(n = 1) + \mathrm{H}_3^+$	(16)	[4]

[1] R. K. Janev, D. Reiter and U Samm, Collision processes in low-temperature hydrogen plasmas, Report JUEL-4105 (2003).

[2] R. K Janev et al., Elementary processes in Hydrogen-Helium plasmas, (Berlin: Springer 1987)

[3] W. L. Wiese, and J. R. Fuhr, Accurate atomic transition probabilities for H, He, Li, J. Phys.. Chem. Ref. Data **38** 565 (2009).

[4] P. del Mazo-Sevillano, ..., D.-H. Kwon, O. Roncero, Molecular physics e2183071

- The cross sections for electron collisions and radiative transitions of D species were used by those of H species. The heavy particle collision cross section of D species was from the ab-initio calculation for D [4]. The mass effect for rate coefficients and mobility of D were taken into account.

$$\alpha(T_{12}) = \frac{4}{\sqrt{\pi} v_{T_{12}}^3} \int_0^\infty \sigma(v_{12}) exp\left(\left(v_{12}/v_{T_{12}}\right)^2\right) v_{12}^3 dv_{12}$$

$$T_{12} = (m_2 T_1 + m_1 T_2)/(m_1 + m_2)$$

$$v_{T_{12}} = \sqrt{2(m_1 + m_2) T_{12}/m_1 m_2}$$

CRM for H/D plasma

For atomic levels n_i $(i = 1 - 40)$

$$D_{\mathrm{AH}^+} = T_e K_1^0 \left(\frac{760}{p}\frac{T_m}{273}\right)$$

$$p = n_{\mathrm{H}_2} T_m$$

$$K_1^0 = 15.9\ (\mathrm{H}^+), 11.2 (\mathrm{D}^+)$$
$$(cm^2 V^{-1} s^{-1})$$

$$D_{\mathrm{AH}^+} : D_{\mathrm{AH}_2^+} : D_{\mathrm{AH}_3^+} = 1 : \frac{\sqrt{2}}{\sqrt{3}} : \frac{\sqrt{5}}{3}$$

$$\frac{dn_i}{dt} = \sum_{j>i}^{40} \eta_{ji} A_{ji} n_j - \left(\sum_{j<i} \eta_{ij} A_{ij} + \frac{Q}{V} + \frac{\gamma}{\tau}\delta_{i1}\right) n_i +$$
$$n_e\left(\sum_{j\neq i} \beta_{1,ji}\, n_j - \sum_{j\neq i} \beta_{1,ij}\, n_i - \beta_{2i} n_i + \beta_{4i}\, n_{\mathrm{H}^+}\right) +$$
$$n_e(\beta_{5i} + \beta_6 \delta_{i2} + \beta_7 \delta_{i1}) n_{41} + n_e(\beta_{9i} + \beta_{10i} + \beta_{12i}) n_{42} +$$
$$n_e(\beta_{13}\delta_{i1} + \beta_{14}\delta_{i2} + \beta_{15}\delta_{i1}) n_{43} + n_{41}\beta_{16}\delta_{i1} n_{42} +$$
$$\left(\sum_{j=42}^{43} \varsigma_{aj} \left(\frac{\mu}{R}\right)^2 D_{Aj} n_j + \varsigma_{aD^+} \left(\frac{\mu}{R}\right)^2 D_{\mathrm{AH}^+} n_{\mathrm{H}^+}\right) \delta_{i1}$$

$$\tau = 2R/v_{th}$$

$$v_{th} = 2\sqrt{\frac{2T_a}{\pi M_H}}$$

$$\mu = 2.405$$

For molecule and ions n_i (i=41,42,43 for H_2, H_2^+, H_3^+)

$$\frac{dn_i}{dt} = \delta_{i41}\left(n_e \beta_{14} n_{43} + \frac{Q_{in}}{V} \times 4.48 \times 10^{17} + \frac{\gamma'}{\tau} n_1 + \sum_{j=42}^{43} \varsigma_{mj} \left(\frac{\mu}{R}\right)^2 D_{Aj} n_j + \varsigma_{m\mathrm{H}^+} \left(\frac{\mu}{R}\right)^2 D_{AH^+} n_{\mathrm{H}^+}\right)$$
$$-\delta_{i41} n_e(\beta_5 + \beta_6 + \beta_7 + \beta_8) n_i - \delta_{i42} n_e (\beta_9 + \beta_{10} + \beta_{11} + \beta_{12}) n_i -$$
$$\delta_{i43} n_e (\beta_{13} + \beta_{14} + \beta_{15}) n_i + \delta_{i42}(n_e \beta_8 - n_{41}\beta_{16}) n_i +$$
$$n_{41}\beta_{16}\delta_{i43} n_{42} - \delta_{i41}\beta_{16} n_{42} n_i - \frac{Q}{V} n_i - (1 - \delta_{i41}) \left(\frac{\mu}{R}\right)^2 D_{Ai} n_i$$

Quasi neutrality condition for H^+ ion n_{H^+} : $\boldsymbol{n_e = n_{\mathrm{H}^+} + n_{\mathrm{H}_2^+} + n_{\mathrm{H}_3^+}}$

rather than **pressure balance equation** :

$$p_{tot} = n_m k_B T_m + k_B T_a \left(\sum_{j=1}^{40} n_j + n_{\mathrm{H}^+}\right) + n_e k_B T_e + n_m k_B \left(n_{\mathrm{H}_2^+} + n_{\mathrm{H}_3^+}\right)$$

Results for H/D CRM

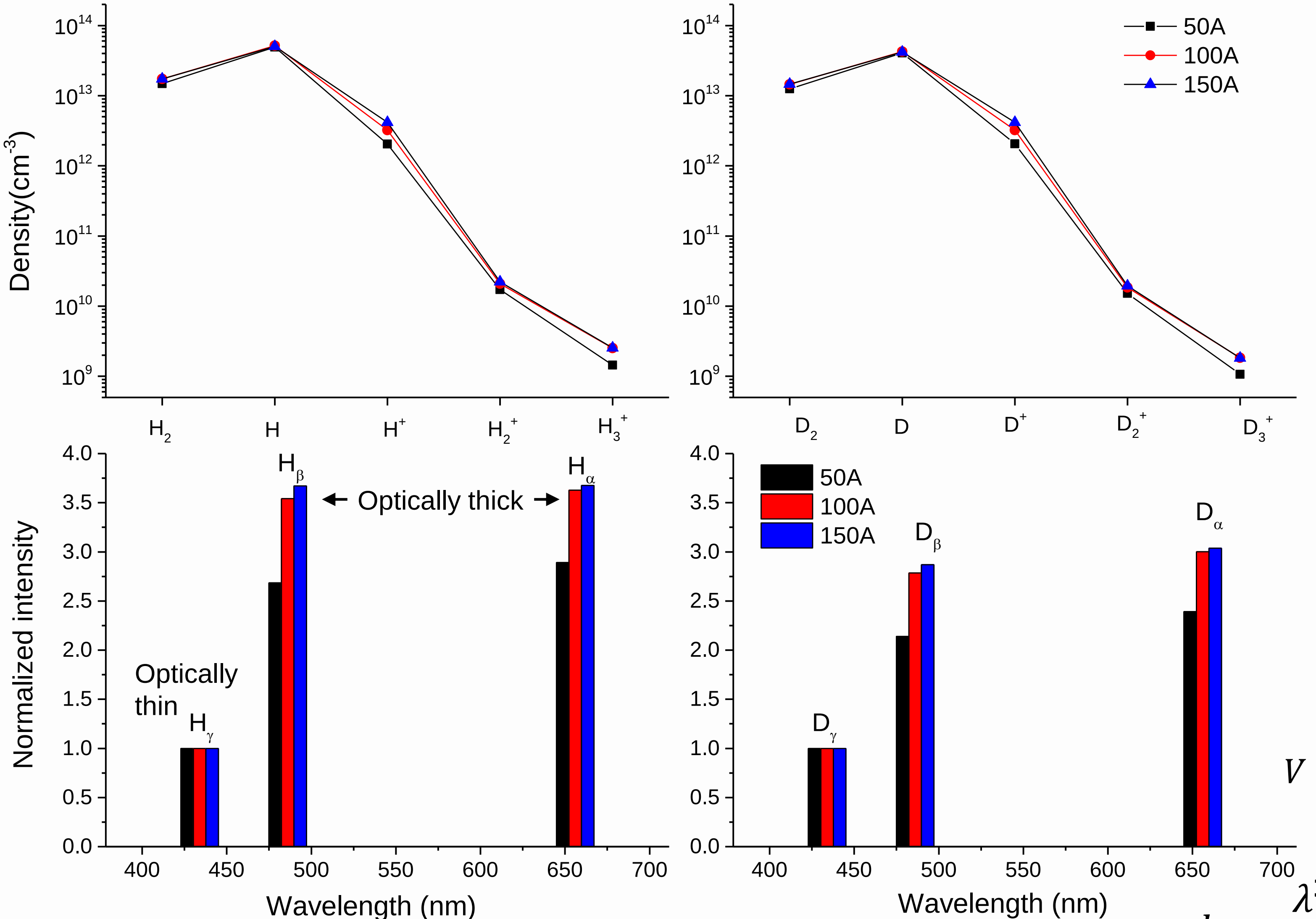

$T_m = 300\text{K},$
$T_a = 600\text{K},$
$R_{eff} = 40\ \text{cm},$

$T_e = 5.55\ (50\text{A}),$
$4.68\ (100\text{A}),$
$4.66\ (150\text{A})\ \text{eV}$

$n_e = 2.07\ (50A),$
$3.25\ (100\text{A}),$
$4.18\ (150\text{A}),$
$\times\ 10^{12} (\text{cm}^{-3})$

$Q_{in} = 600\ \text{sccm},$
$Q = 4800\ \text{lps},$

$V = 2.64 \times 10^6 \text{cm}^3,$
$R = 75\ \text{cm}$

$$k_0 = \frac{\lambda^3 N_i}{8\pi} \frac{g_j}{g_i} \sqrt{\frac{A_{ji} M}{2\pi k_B T_g}}$$

$\text{H} \rightarrow \text{D}$, $k_0 \uparrow \eta \downarrow$

Sensitivity to used atomic data ($X_2 + X_2^+, X = H, D$)

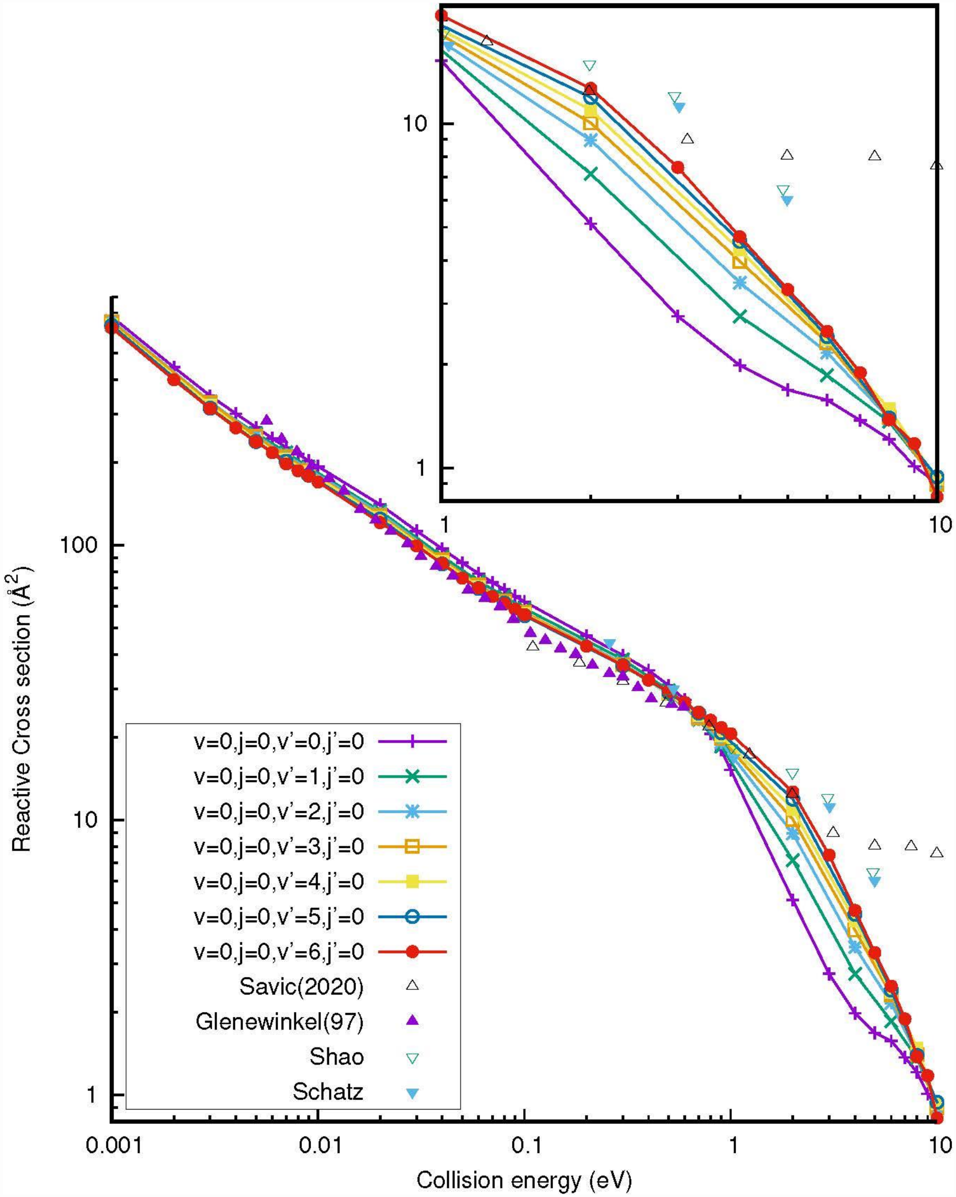

Recent data for

$$H_2(v = 0, j = 0) + H_2^+(v', j' = 0) \\ \rightarrow H_3^+ + H$$

reactive cross sections obtained with QCT (quasi-classical trajectory) calculations

P. del Mazo-Sevillano, …, D.-H. Kwon, O. Roncero, "Vibrational, non-adiabatic and isotopic effects in the dynamics of the $H_2 + H_2^+ \rightarrow H_3^+ + H$ reaction: application to plasma modeling", Molecular physics e2183071 (2023) (https://doi.org/10.1080/00268976.2023.2183071)

Comparisons of used atomic data

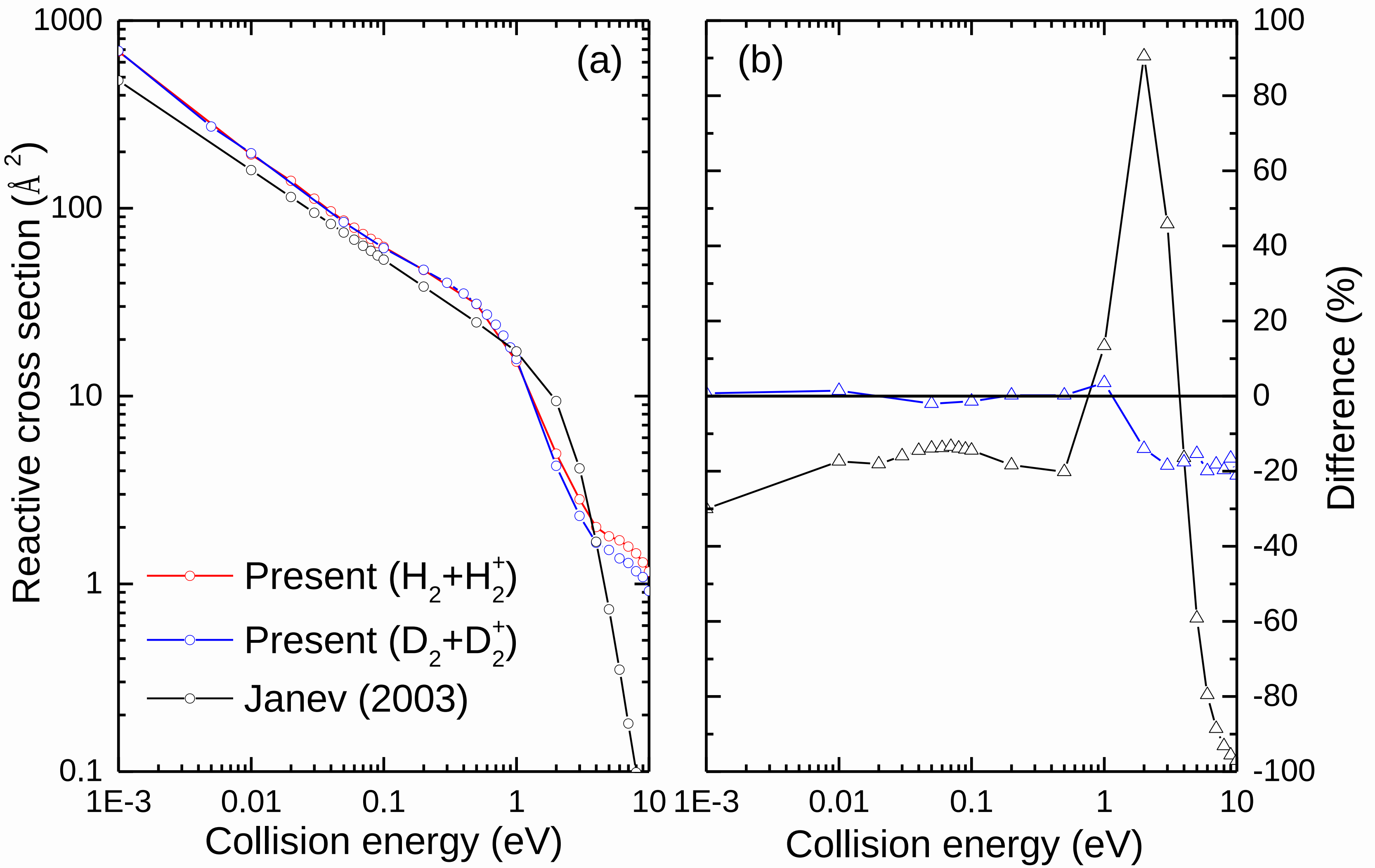

Resulting populations

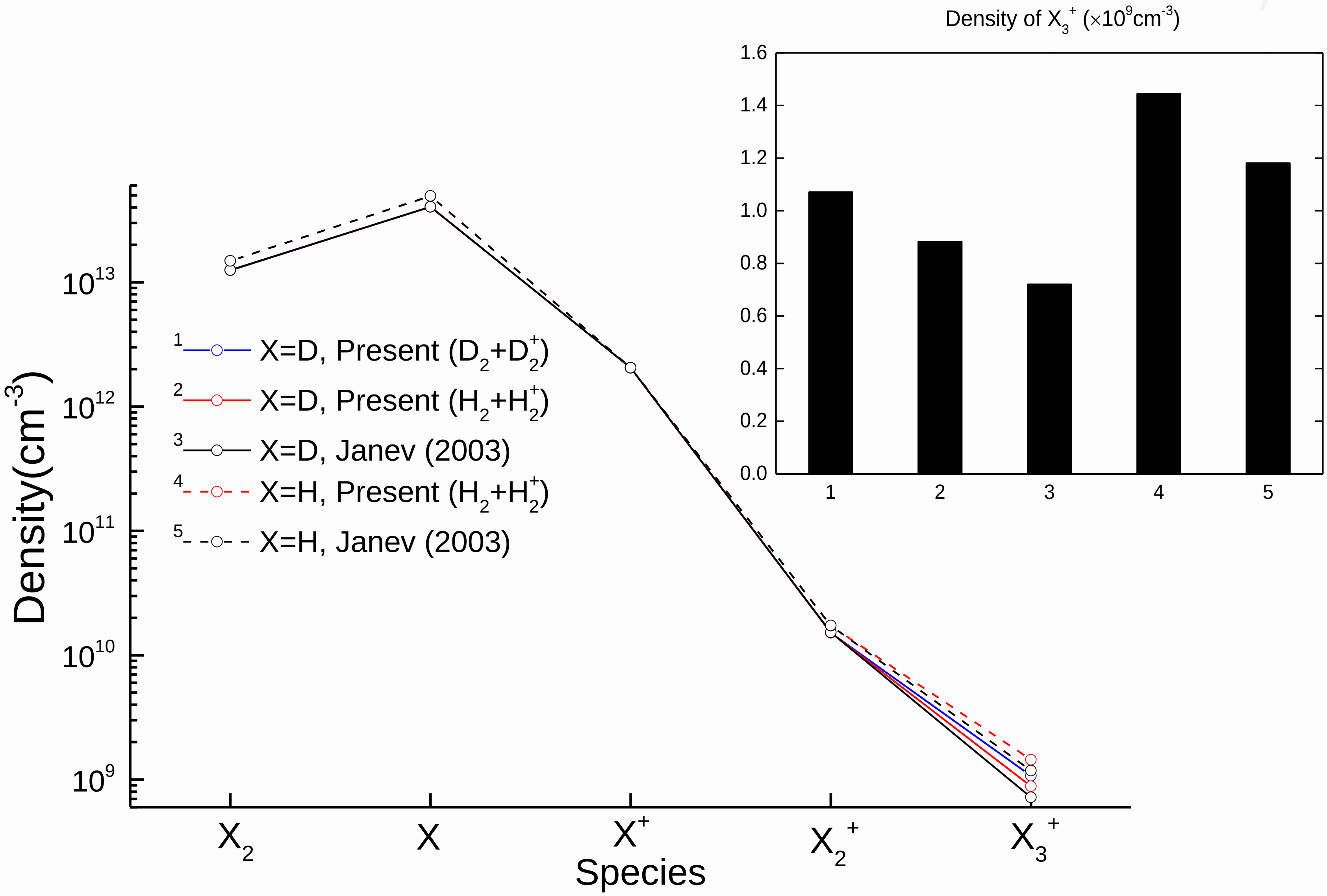

H_3^+ dominant case

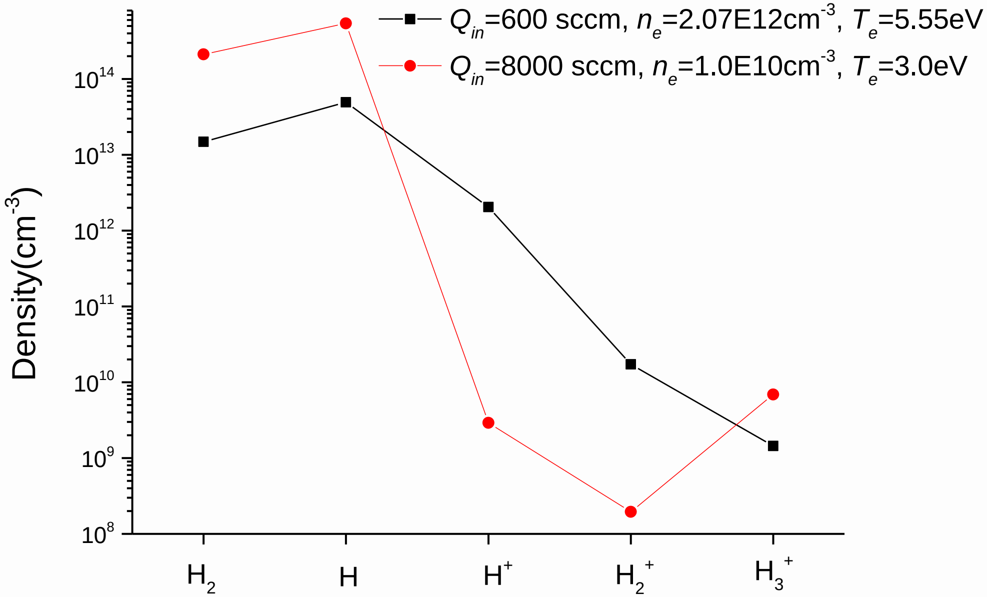

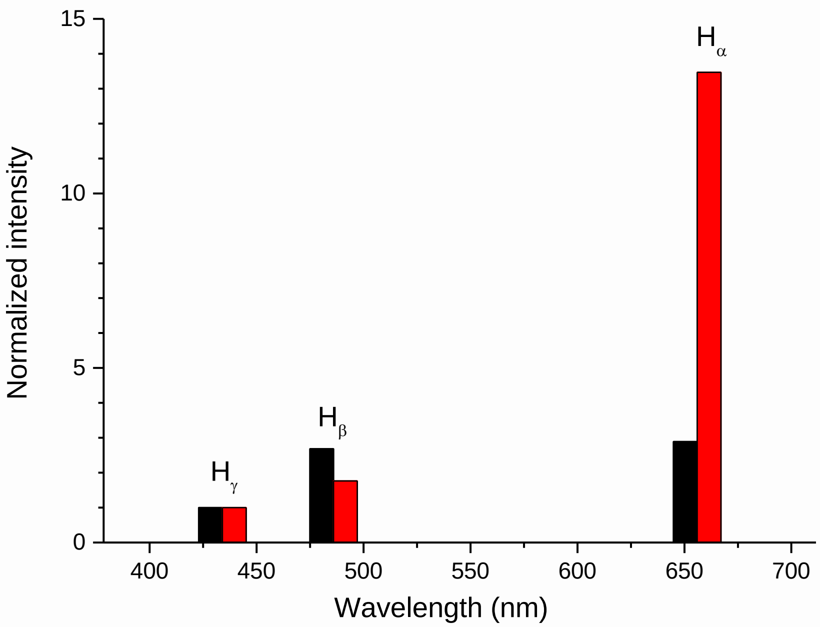

Sensitivity to used atomic data ($X_2 + \mathrm{e}, X = \mathrm{H}, \mathrm{D}$)

$$X_2 + e \rightarrow X(n) + X(n') + e$$

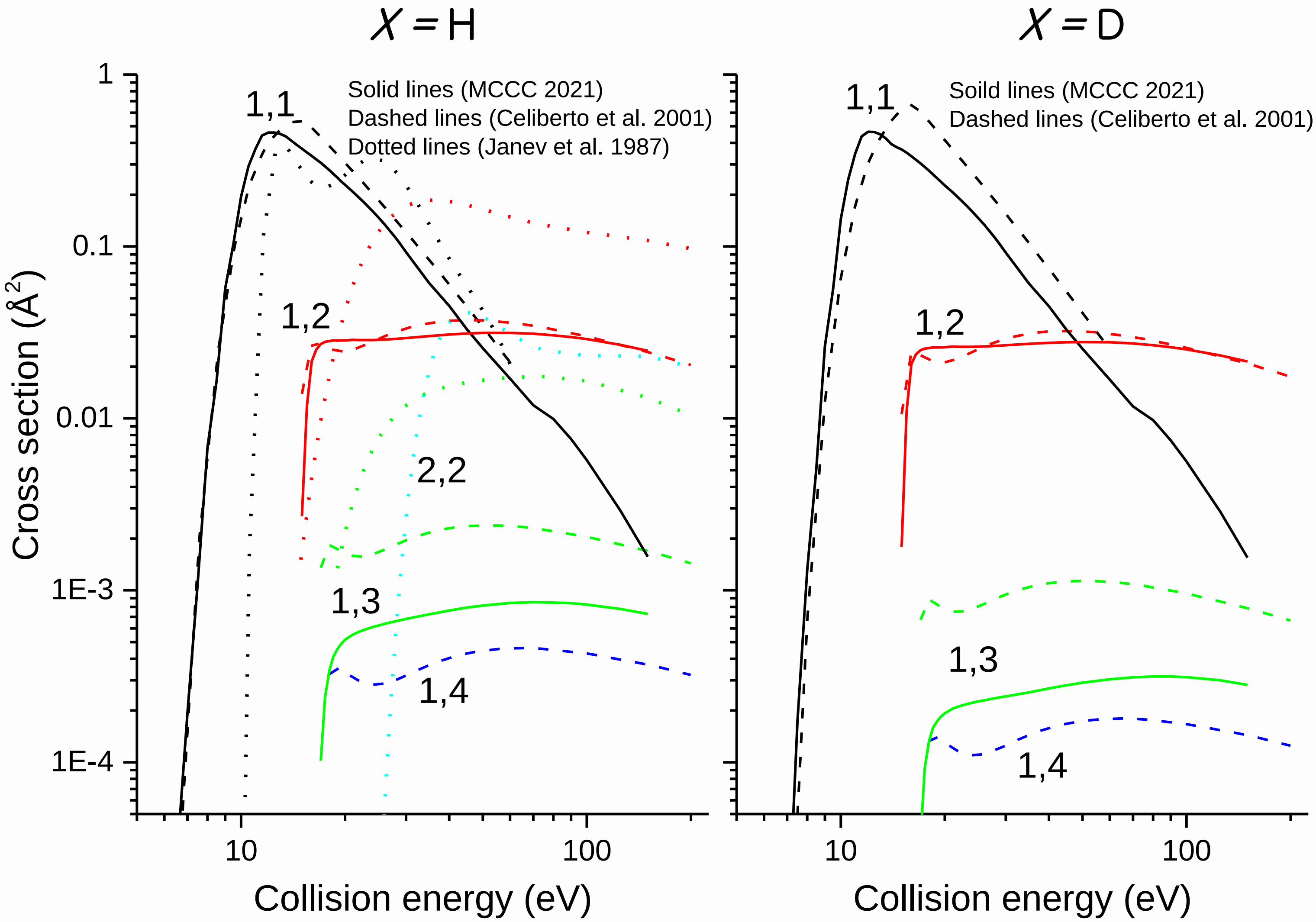

R. Celiberto et al., Atom. Data Nucl. Data Tables **77** 161 (2001).

L. H. Scarlett, D. Fursa et al., Atom. Data Nucl. Data Tables, **137** 101361 (2021).

H molecular energy levels

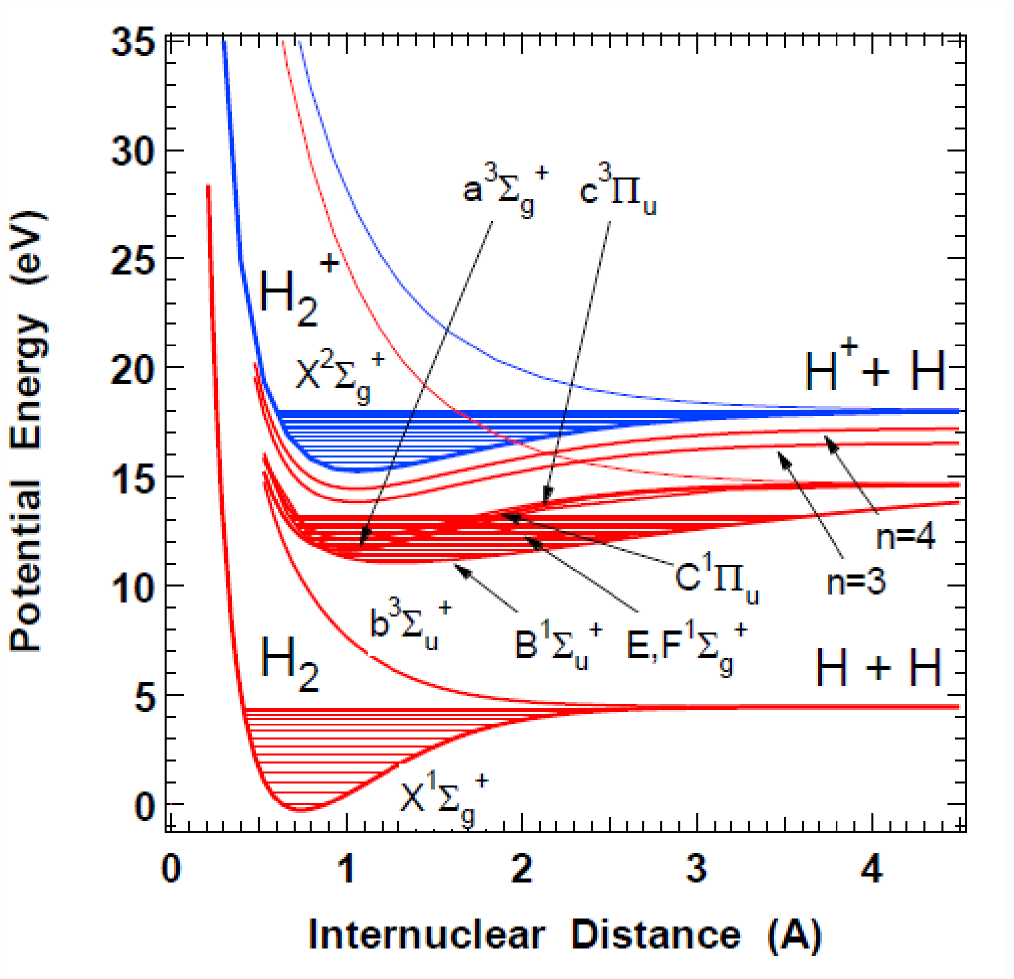

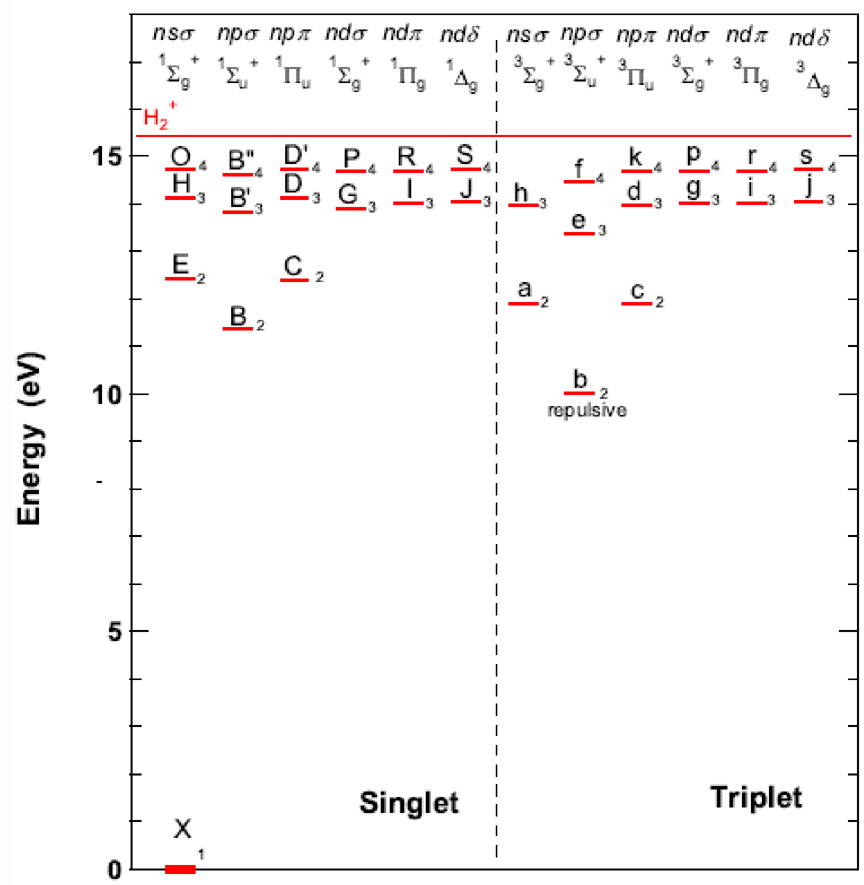

K. Sawada and M. Goto, Atoms **4** 29 (2016)

Comparisons of used atomic data

$$X_2 + e \rightarrow X(n = 1) + X(n' = 1) + e$$

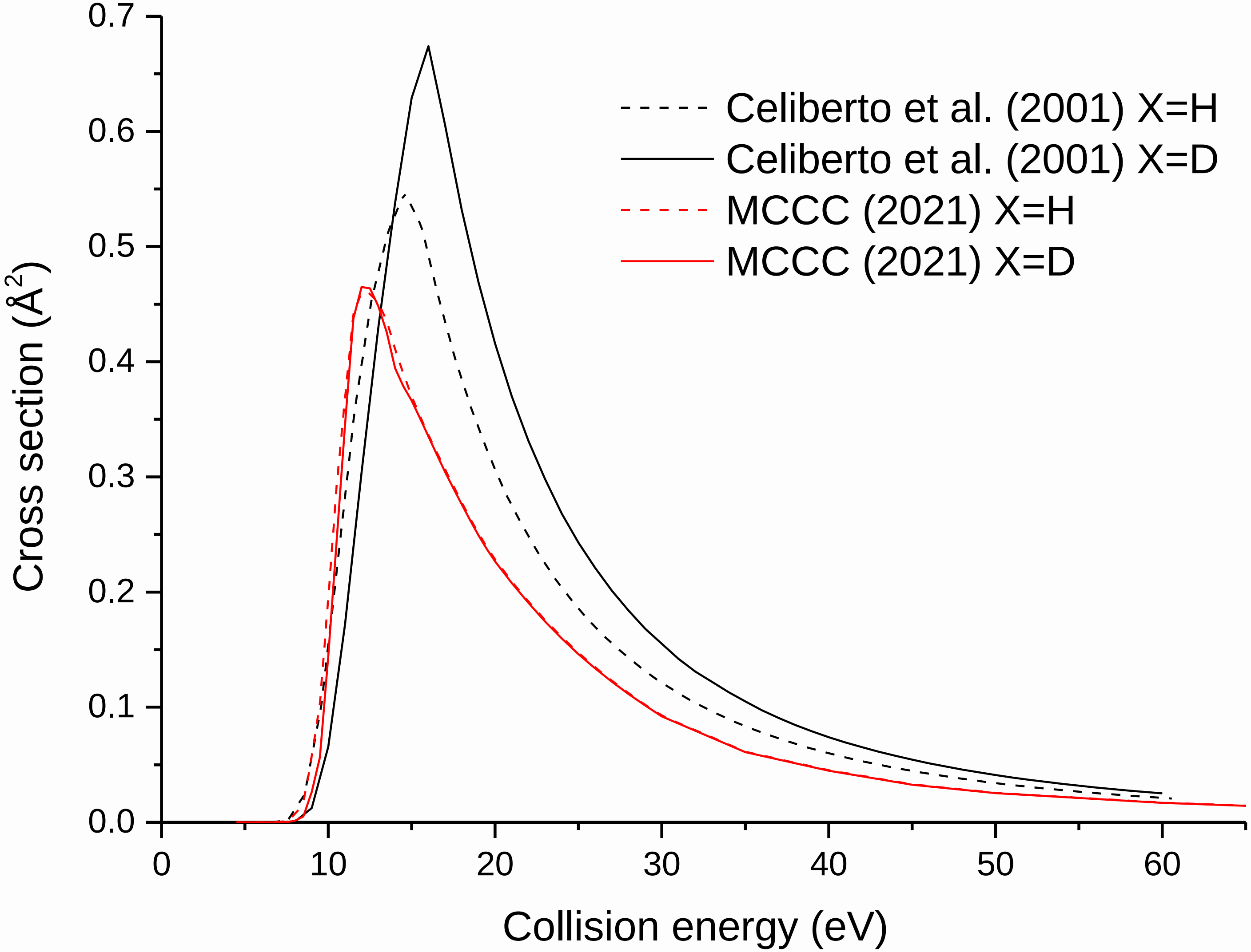

Comparisons of used atomic data

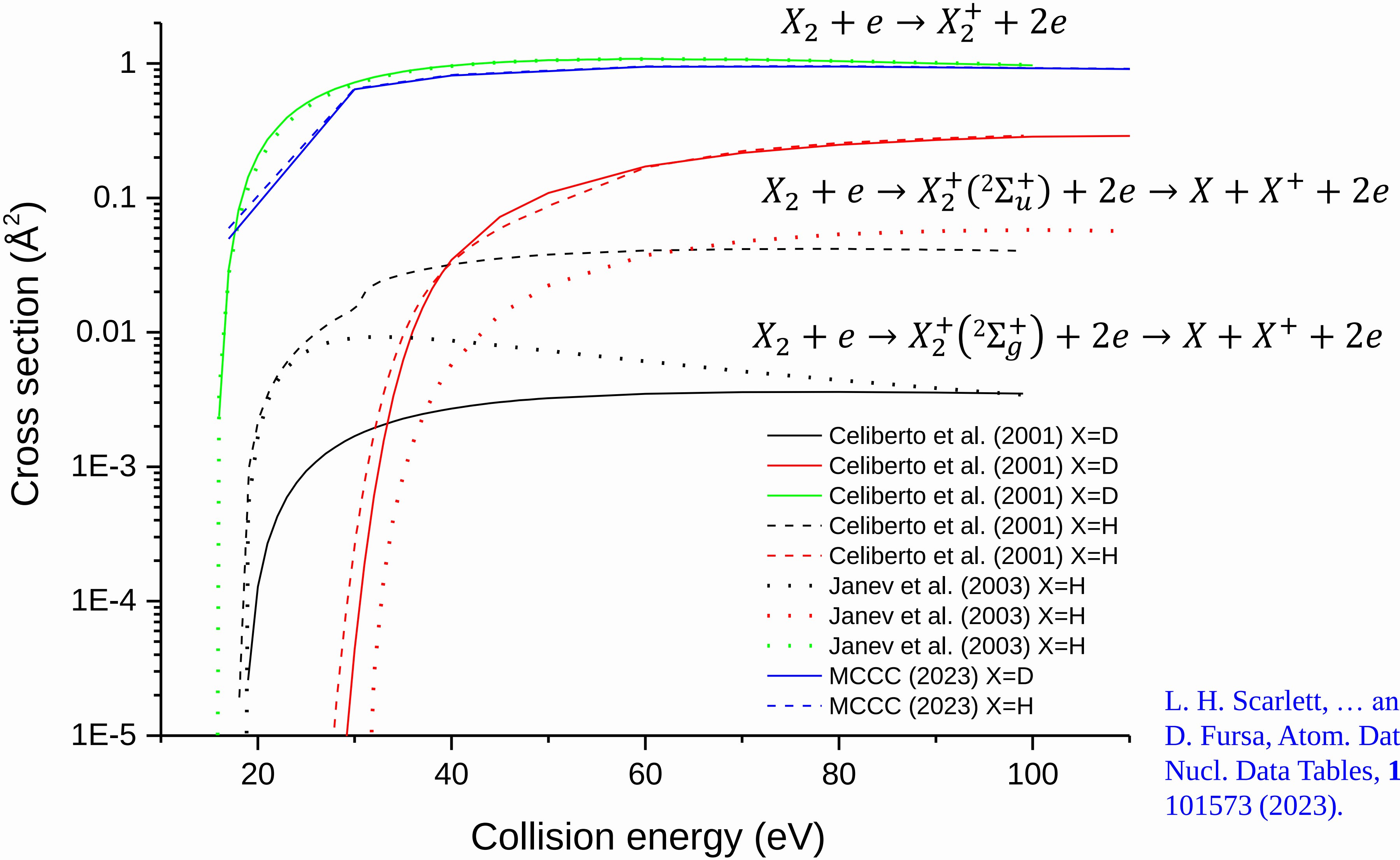

L. H. Scarlett, … and D. Fursa, Atom. Data Nucl. Data Tables, **151** 101573 (2023).

Comparisons of used atomic data

$$X_2 + e \rightarrow X_2^+ + 2e$$

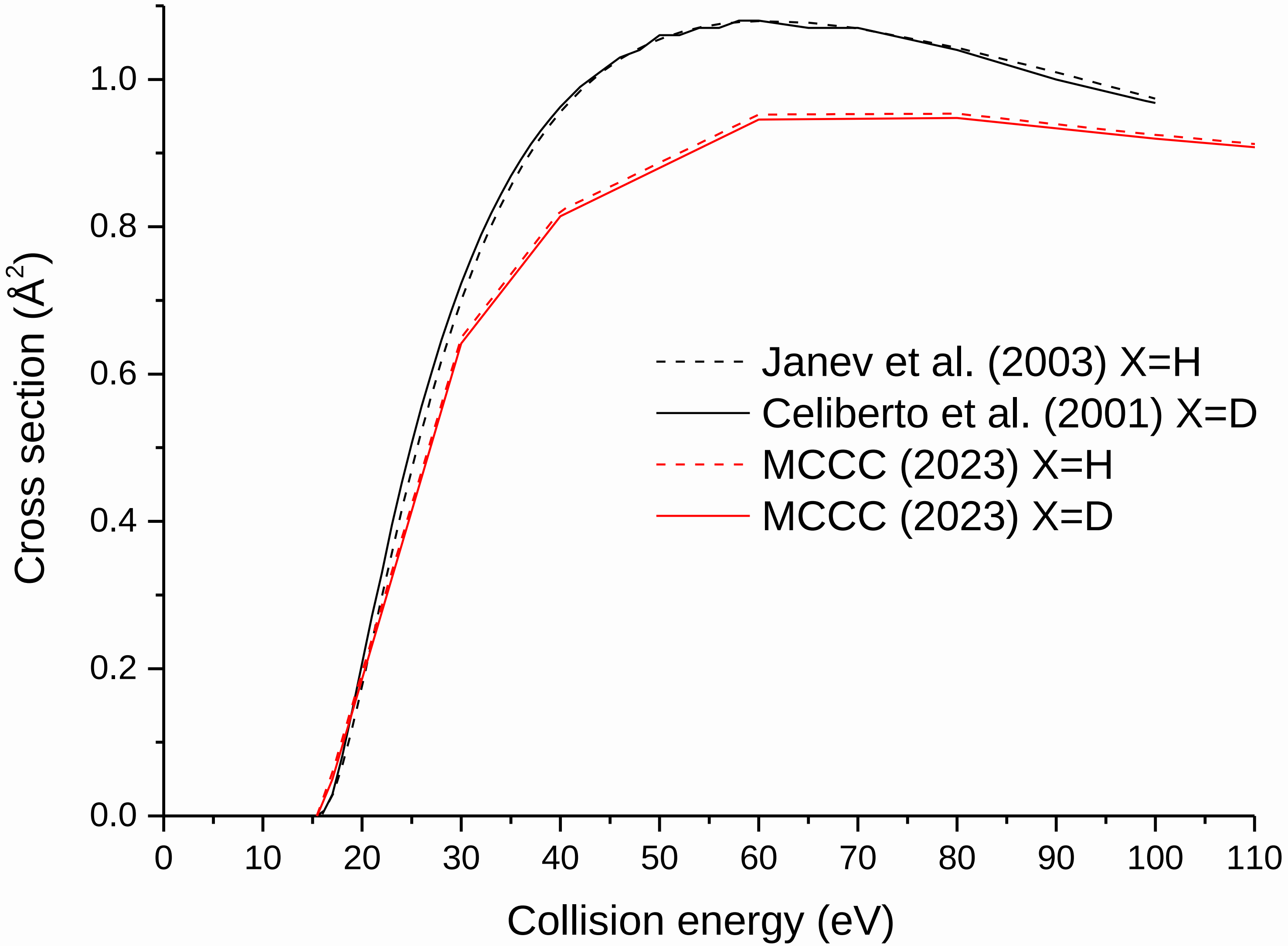

Resulting populations and spectra

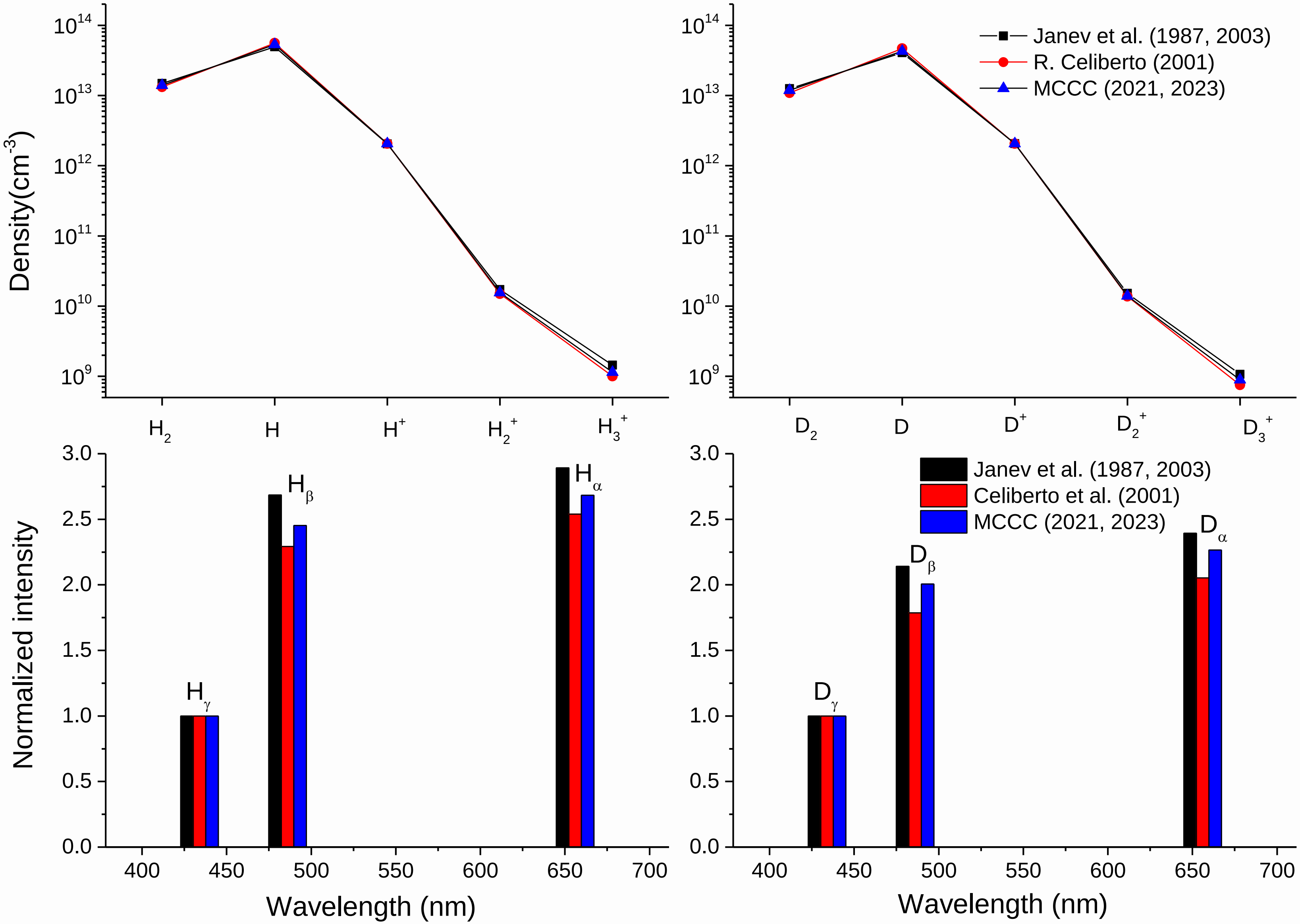

Sensitivity to plasma parameters n_e and T_e

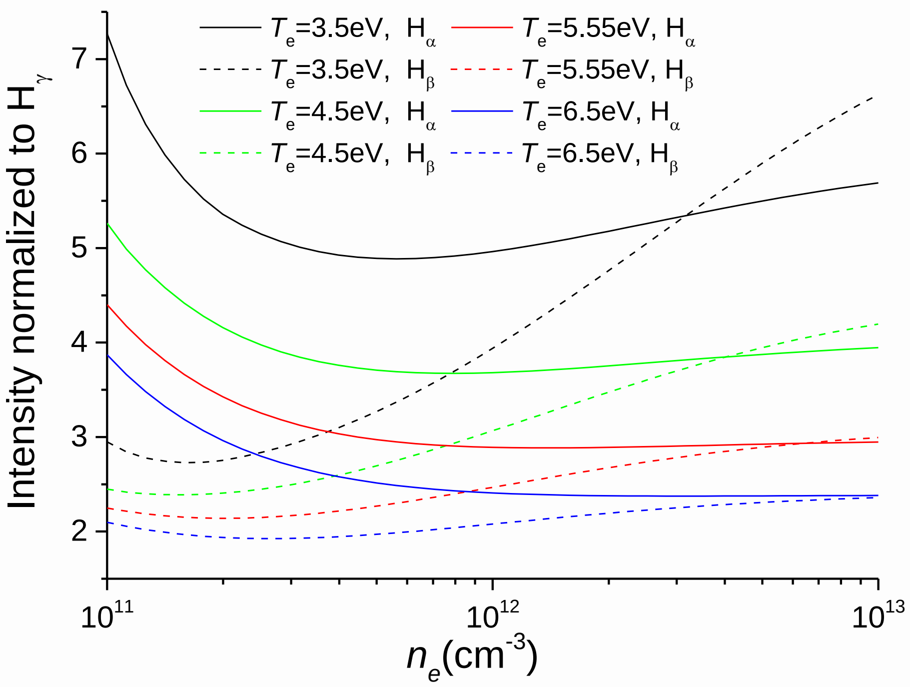

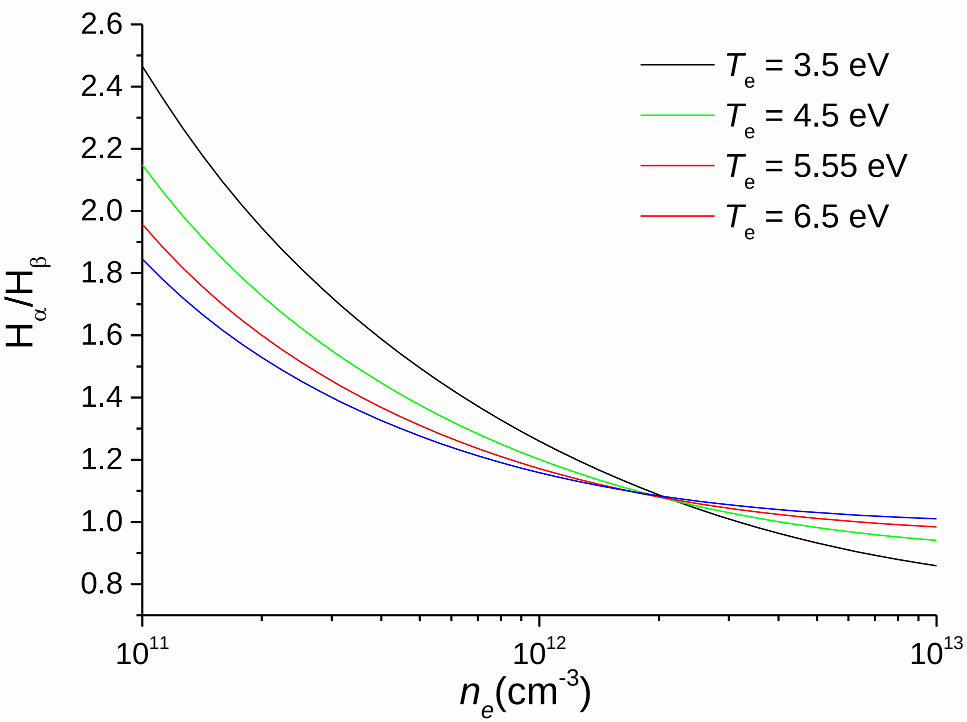

CRM for vibrational states of H molecules

Energy level diagram of H_2

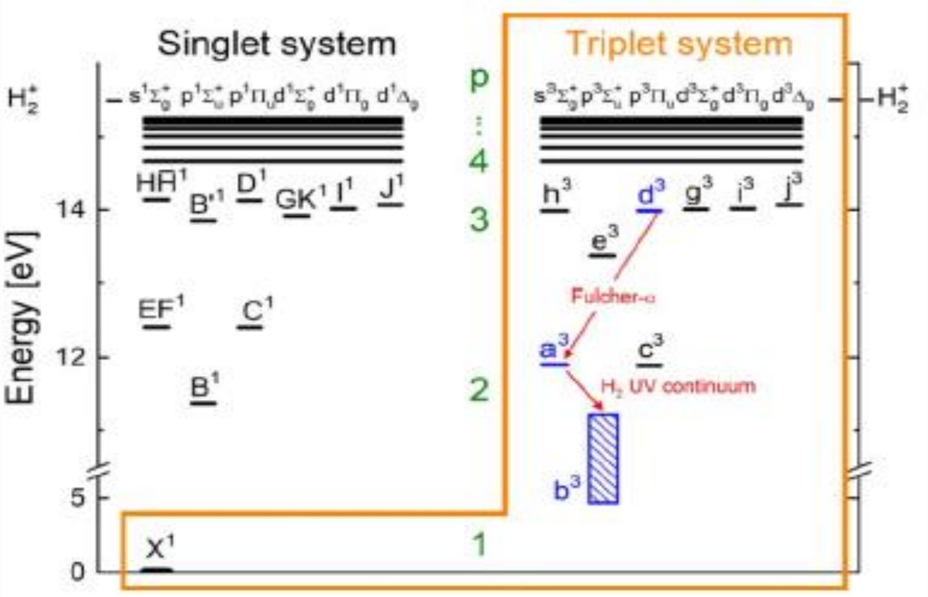

Ref. D. Wünderlich et al., J. Phys. D: Appl. Phys. **54** 115201 (2016)

CRM for molecular spectra

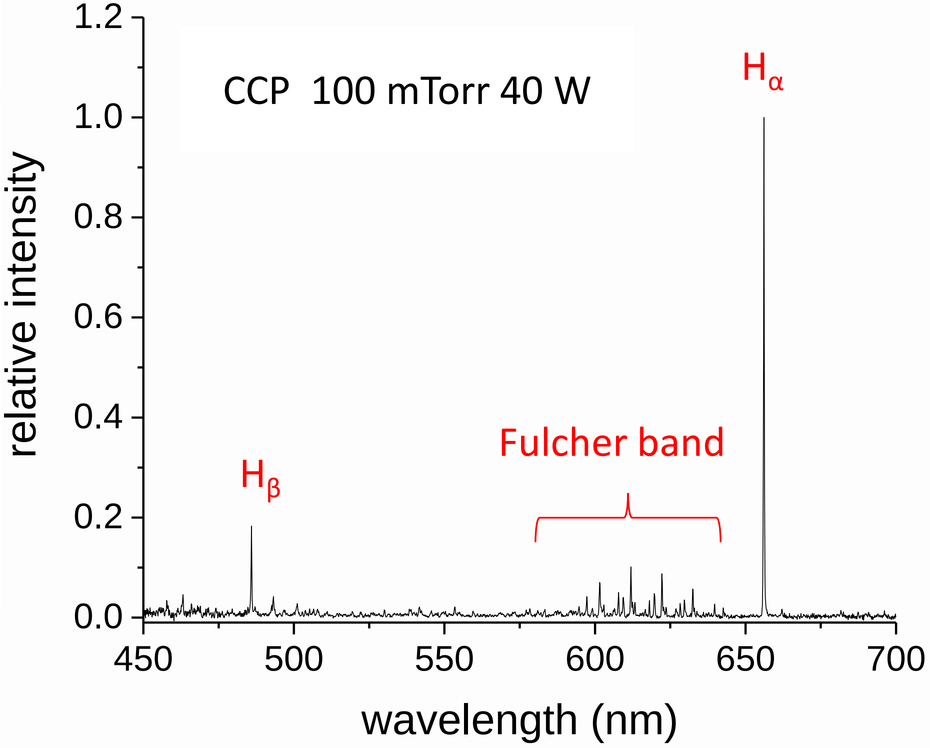

Contents

- Collisional-radiative modeling (CRM) for He, H/D plasmas
  - Modeling methods and AM data
  - Sensitivities to used AM data and plasma parameters

- S/XB ratio for sputtering yield of W
  - S/XB ratio methods and atomic data
  - Experimental S/XB ratios

S/XB ratio for sputtering yield

$$\Gamma = \int n_e S_{Z\rightarrow Z+1} N_Z dx = \int n_e \frac{S_{Z\rightarrow Z+1}}{\frac{n_i}{N_Z} A_{ij}} \left(\frac{n_i}{N_Z} A_{ij}\right) N_Z \, dx$$

$$= \int \frac{\sum_\sigma n_\sigma S_\sigma / N_Z}{\sum_\sigma n_\sigma q_{\sigma i} / N_Z \cdot A_{ij} / \sum_{k<i} A_{ik}} n_i A_{ij} dx = \frac{S}{XB} I$$

$$S_{Z\rightarrow Z+1} N_Z = \sum_\sigma S_\sigma n_\sigma$$

$$n_i \sum_{k<i} A_{ik} = n_e \sum_\sigma n_\sigma q_{\sigma i}$$

$$N_Z = \sum_\sigma n_\sigma,$$

$$\frac{S}{XB} \qquad I = \int n_i A_{ij} dx$$

$$\Gamma_{\mathrm{W}}^{\mathrm{Spt}} = \Gamma_{\mathrm{W}^+} + \Gamma_{\mathrm{W}}^{\mathrm{GL}}$$

$$\Gamma_{\mathrm{W}}^{\mathrm{Spt}} \approx \Gamma_{\mathrm{W}^+} = 4\pi \frac{S}{XB} I_{\mathrm{WI}}$$

$$\frac{S}{XB} = \frac{\Gamma_{\mathrm{W}}^{\mathrm{Spt}}}{4\pi I_{\mathrm{WI}}} = \frac{Y\Gamma_i}{4\pi I_{\mathrm{WI}}}$$

Schematic diagram for optical diagnostic in KPBIF

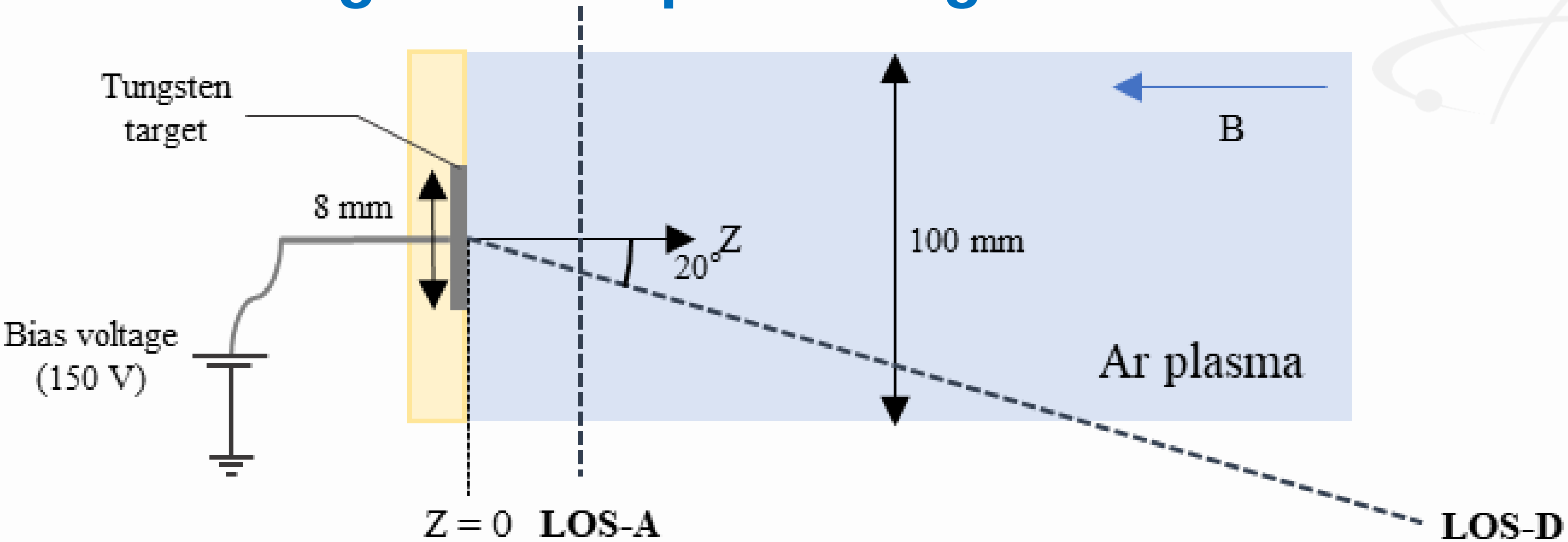

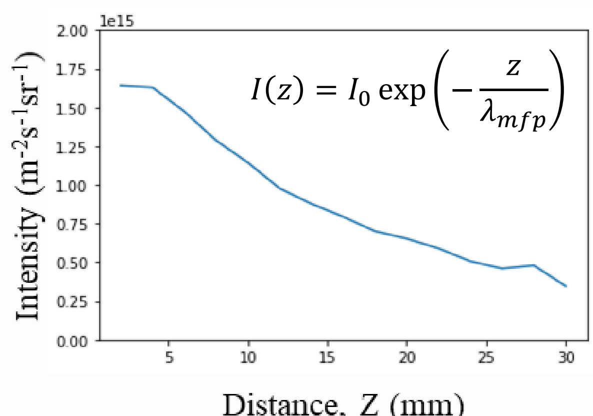

$$\frac{\Gamma_{\mathrm{W}}^{\mathrm{GL}}}{\Gamma_{\mathrm{W}}} = \exp\left(-\frac{L}{\lambda_{mfp}}\right)$$

$$\frac{\Gamma_{\mathrm{W}^+}}{\Gamma_{\mathrm{W}}} = 1 - \exp\left(-\frac{L}{\lambda_{mfp}}\right)$$

$$\frac{S}{XB} = \frac{\Gamma_{\mathrm{W}^+}}{4\pi I_{\mathrm{WI}}} = \frac{Y\Gamma_i}{4\pi I_{\mathrm{WI}}} \times \left\{1 - \exp\left(-\frac{L}{\lambda_{mfp}}\right)\right\}$$

D. Nishijima et al., "Experimental determination of S/XB values of W I visible lines." Phys. Plasmas **16** 122503 (2009)

Correction factor for the geometrical loss

$$\frac{dN_{\mathrm{W}}(x)}{dx} = -\frac{1}{\lambda_{mfp}} N_w(x)$$

$$\frac{dN_{\mathrm{W}}(x)}{dt} = -RC(T_e)n_e N_{\mathrm{W}}(x), \quad \frac{dt}{dx} = \frac{1}{V_{\mathrm{W}}}$$

$$\lambda_{mfp} = \frac{V_{\mathrm{W}}}{RC(T_e)n_e}$$

Sputtering yield of W by Ar ion beam

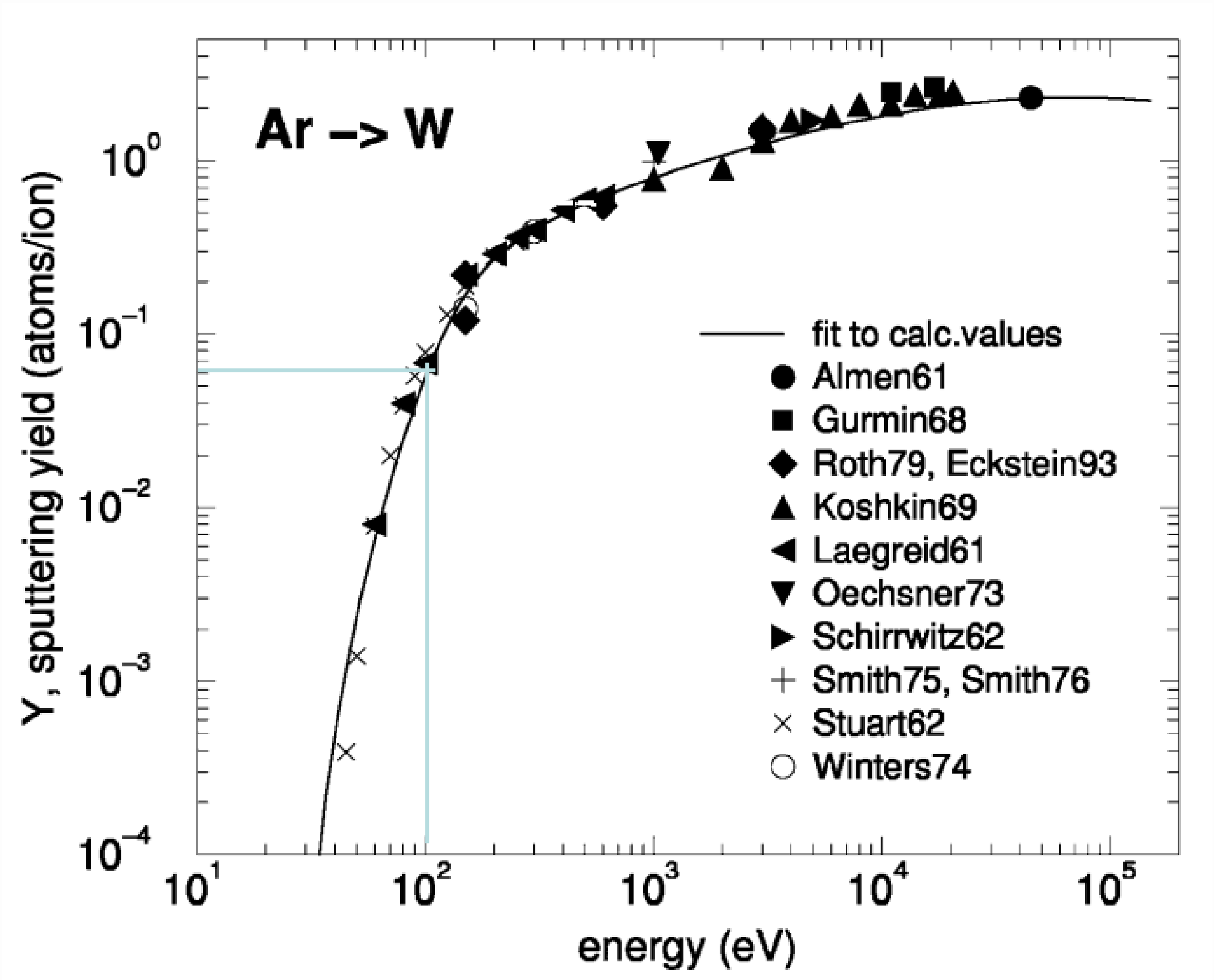

Y=0.06 at 100 eV

W. Eckstein, "Sputtering by Particle Bombardment", Springer-Verlag, Berlin (2007)

Measured S/XB ratios

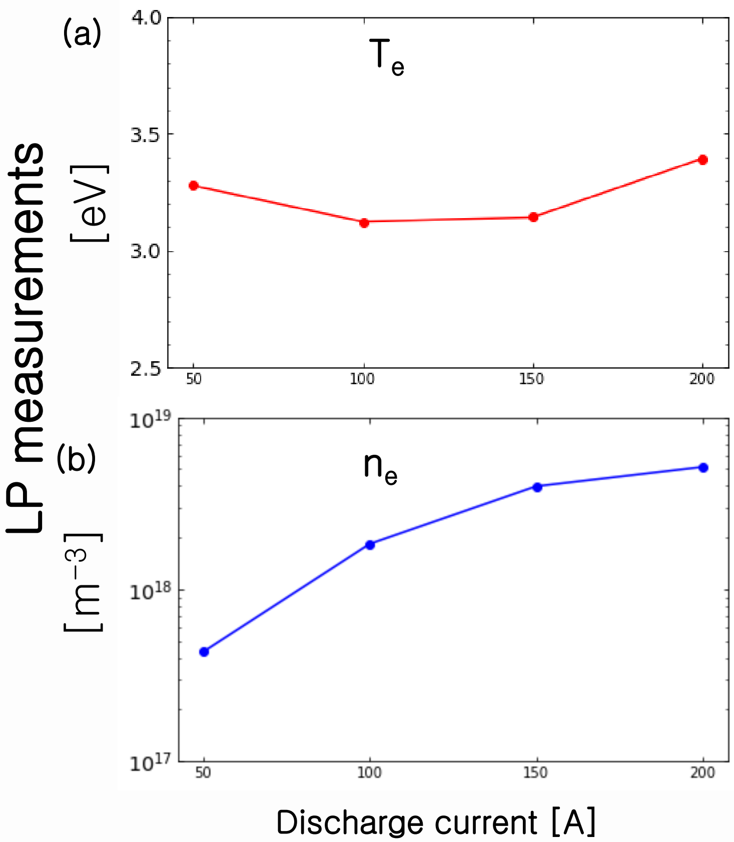

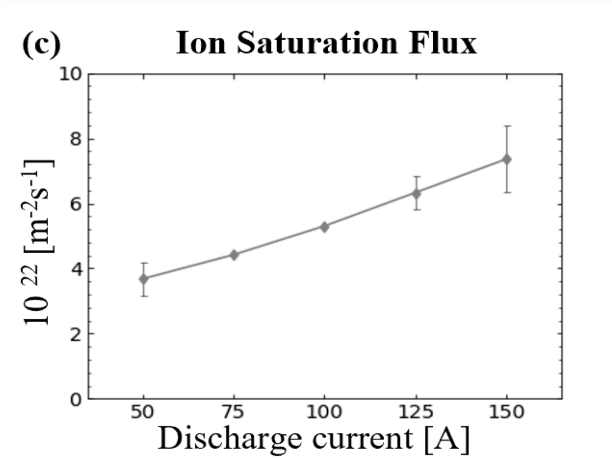

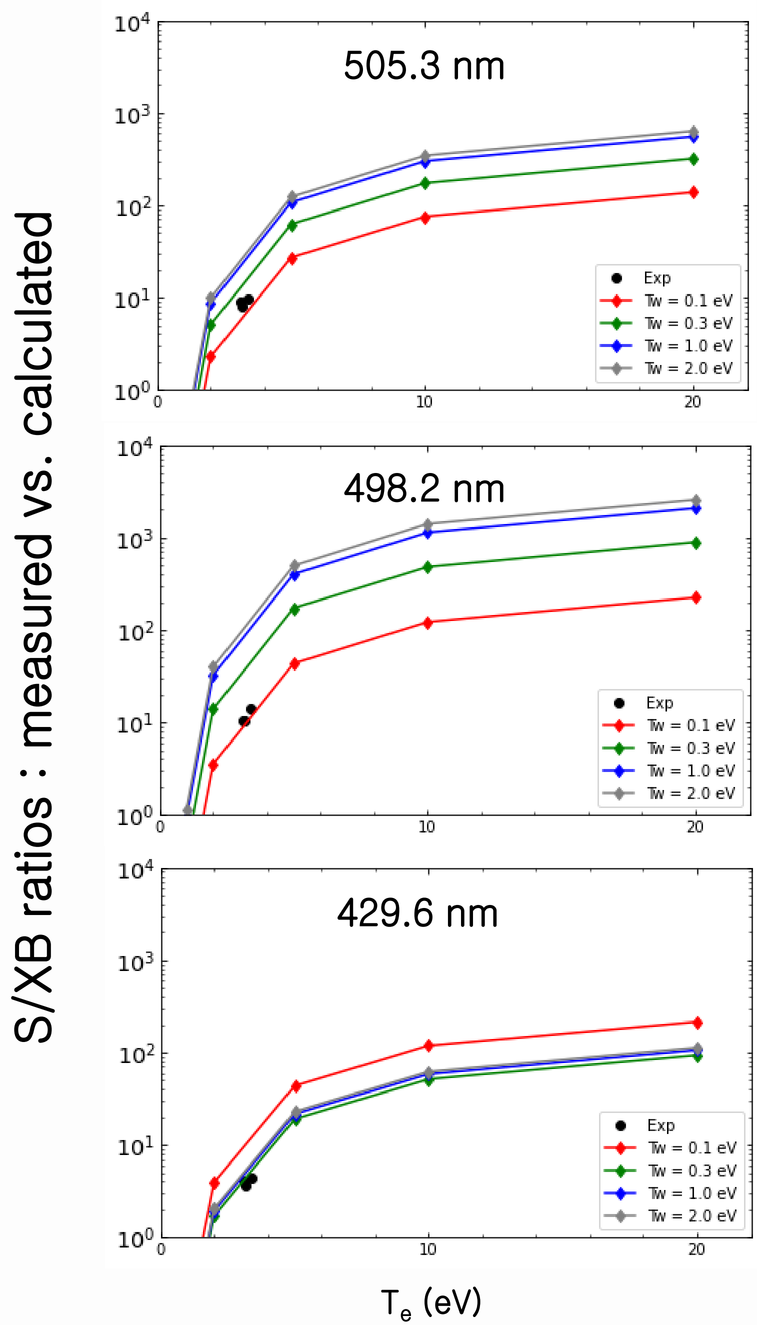

Calculated data

I. Beigman et al., “Tungsten spectroscopy for the measurement of W-fluxes from plasma facing components”, Plasma Physics and Controlled Fusion **49** 1833 (2007)

Calculations of S/XB by I. Beigman et al. (2007)

Electron impact ionization (EII) rate

$$\langle v\ \sigma_{iz}\rangle = 10^{-8} A \frac{\sqrt{\beta}(\beta+1+D)}{(\beta+\chi)(\beta+1)\sqrt{\beta_{iz}+1}} e^{-\beta_{iz}} (\mathrm{cm^3 s^{-1}})$$

$$\beta = Ry/T_e,\ \beta_{iz} = E_{iz}/T_e,\ \ E_{iz} = 7.9\ \mathrm{eV}, \qquad A = 84.9, \chi = 0.22, D = -0.4$$

for the 6s and 5d shells by Born-Ochkur approximation using ATOM

Electron impact excitation (EIE) rate

$$\langle v\ \sigma_{k_0 k}\rangle = 0.11 \times 10^{-16} \frac{g_k}{g_{k_0}} A_{k k_0} \left(\frac{Ry}{\Delta E}\right)^3 u(T_e) e^{-\beta_{ex}} (\mathrm{cm^3 s^{-1}})$$

$$u(T_e) = \beta^{0.5} \log\left(2 + \frac{1}{1.78\beta_{ex}}\right),\ \beta = Ry/T_e,\ \ \beta_{ex} = \Delta E/T_e$$

for the dipole transitions by the semi-empirical van Regemorter formula (Astrophys. J. **136** 906 (1962))

The ionization per photon

$$\frac{S}{XB} = \langle v\ \sigma_{iz}\rangle / \sum_{k_0} N_{k_0} \langle v\ \sigma_{k_0 k}\rangle \cdot \sum_{k''} A_{kk''}/A_{kk'}$$

Selected lines for S/XB of W I

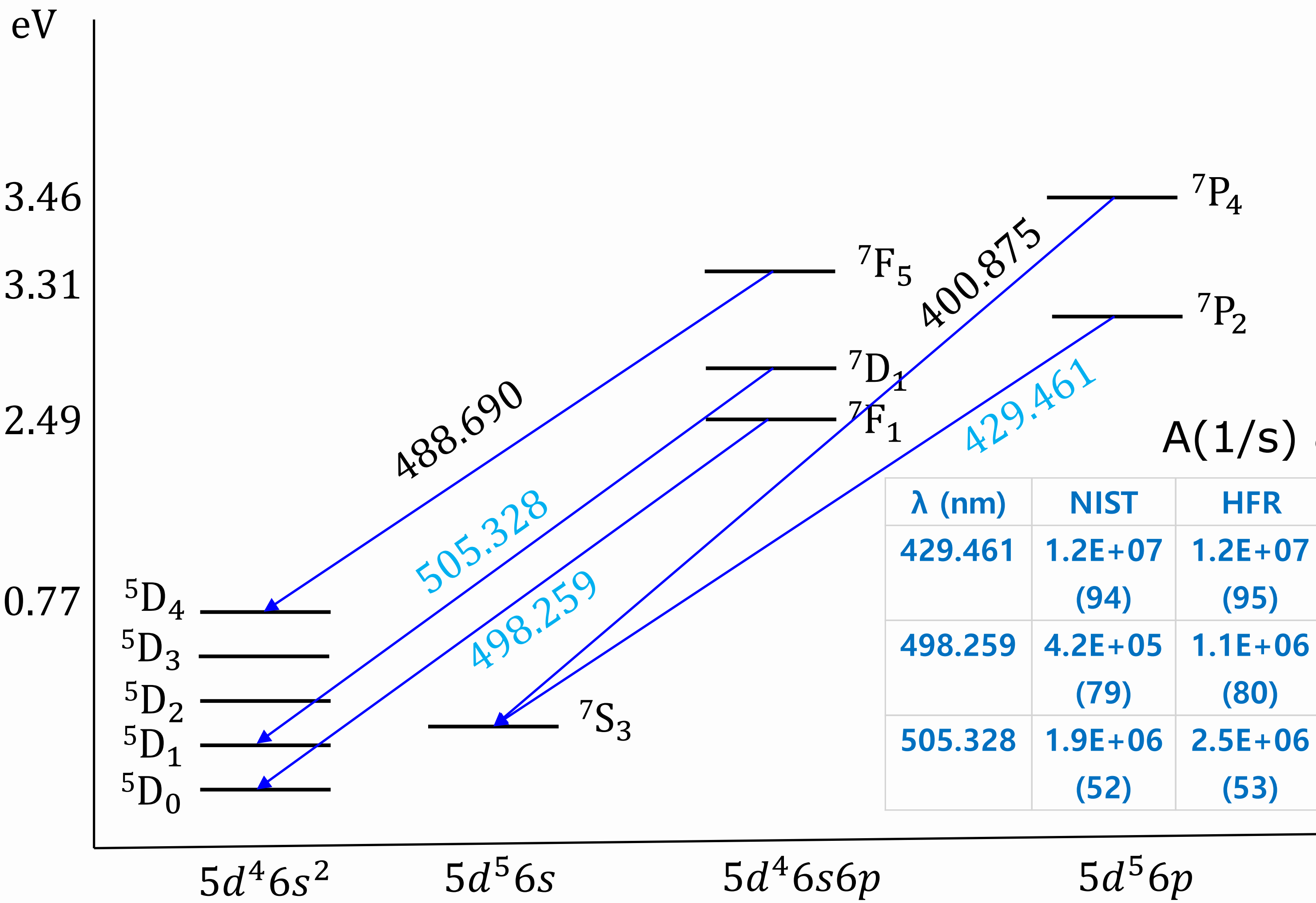

A(1/s) & BR(%)

λ (nm)	NIST	HFR	GRASP	MCDFGME
429.461	1.2E+07 (94)	1.2E+07 (95)	3.2E+07	2.4E+07 (91)
498.259	4.2E+05 (79)	1.1E+06 (80)	2.1E+05	4.9E+04 (96)
505.328	1.9E+06 (52)	2.5E+06 (53)	3.20E+06	1.3E+06 (48)

NIST : A. E. Kramida and T. Shirai , J. Phys. Chem. Ref. Data **35** 423 (2006)
HFR : P. Quinet et al., J. Phys. B: At. Mol. Opt. Phys. **44** 145005 (2011), DESIRE DB
GRASP : R. T. Smyth, C. P. Ballance et al., Phys. Rev. A **97** 052705 (2018)
MCDFGME : Present calculation

Energy levels for S/XB of W I

Energies (eV)

Configuration	Term	J	NIST	HFR	GRASP	MCDFGME
$5d^4 6s^2$	^5D	0	0	0	0	0
		1	0.2071	0.2104	0.1273	0.1465
		2	0.4123	0.4192	0.2927	0.3239
		3	0.5988	0.5998	0.4729	0.5204
		4	0.7711	0.7585	0.6631	0.6941
$5d^5 6s$	^7S	3	0.3659	0.3587	0.4057	0.0751
$5d^4 6s6p$	^7F	1	2.4877	2.4826	2.1842	2.1667
	^7D	1	2.6599	2.6581	2.4292	2.4960
$5d^5 6p$ ($5d^4 6s6p$)	^7P	2	3.2521	3.2584	2.9697	2.9706

Configurations for energies W I

		Even parity		
NIST, HF based on EXP (Kramida et al. 2006)	HFR (Wyart 2010)	HFR (Quinet et al. 2011)	GRASP (Smyth et al. 2018)	MCDFGME (Present)
$5d^46s^2$	$5d^46s^2$	$5d^46s^2$	$5d^46s^2$	$5d^46s^2$
$5d^56s$	$5d^56s$	$5d^56s$	$5d^56s$	$5d^56s$
$5d^6$	$5d^6$	$5d^6$	$5d^6$	$5d^6$
$5d^46p^2$		$5d^46p^2$	$5d^46p^2$	$5d^46p^2$
		$5d^46d^2$	$5d^46d^2$	$5d^46d^2$
$5d^36s6p^2$		$5d^36s6p^2$	$5d^36s6p^2$	$5d^36s6p^2$
				$5d^36s6d^2$
		$5d^26s^26p^2$	$5d^26s^26p^2$	$5d^26s^26p^2$
			$5d^26s^26d^2$	$5d^26s^26d^2$
			$5d^47s^2$	$5d^47s^2$
$5d^46s6d$		$5d^46s6d$	$5d^46s6d$	
		$5d^56d$	$5d^56d$	
$5d^46s7s$		$5d^46s7s$	$5d^46s7s$	
$5d^57s$		$5d^57s$	$5d^57s$	$5d^57s$
$5d^58s$				
$5d^46s7d$				
			$5d^36s^26d$	
			$5d^36d^3$	
			$5d^36s^27s$	
			$5d6s^26d^3$	
			$5p^45d^8$	
			$5p^45d^66s^2$	
			$5p^45d^76s$	

		Odd parity		
NIST, HF based on EXP (Kramida et al. 2006)	HFR (Wyart 2010)	HFR (Quinet et al. 2011)	GRASP (Smyth et al. 2018)	MCDFGME (Present)
$5d^46s6p$	$5d^46s6p$	$5d^46s6p$	$5d^46s6p$	$5d^46s6p$
$5d^56p$	$5d^56p$	$5d^56p$	$5d^56p$	$5d^56p$
$5d^36s^26p$	$5d^36s^26p$	$5d^36s^26p$	$5d^36s^26p$	$5d^36s^26p$
		$5d^36p^3$	$5d^36p^3$	$5d^36p^3$
		$5d^26s6p^3$	$5d^26s6p^3$	$5d^26s6p^3$
		$5d^46s7p$		
		$5d^57p$		
		$5d^46s5f$		
		$5d^55f$		
			$5d^36s^27p$	
			$5p^55d^7$	
			$5p^55d^66s$	

- Our present MCDFGME : **Self-consistent-field (SCF) radial wavefunctions in the configuration interaction (CI)** procedure
- Others : **Fixed radial wavefunctions in the CI procedure**, (GRASP : Extended Average Level (EAL) method)

S/XB for various DB's

$$N_{k_0} = \frac{(2J_{k_0} + 1)\exp(-\Delta E_{k_0}/T_W)}{\sum_k (2J_k + 1)\exp(-\Delta E_k/T_W)}$$

Config.	$5d^4 6s^2$					$5d^5 6s$
Level	$^5D_0$	$^5D_1$	$^5D_2$	$^5D_3$	$^5D_4$	$^7S_3$
N_{k0}, T_w=2eV	0.04	0.11	0.16	0.21	0.25	0.23
N_{k0}, T_w=0.1eV	0.60	0.23	0.05	0.01	0.00	0.11

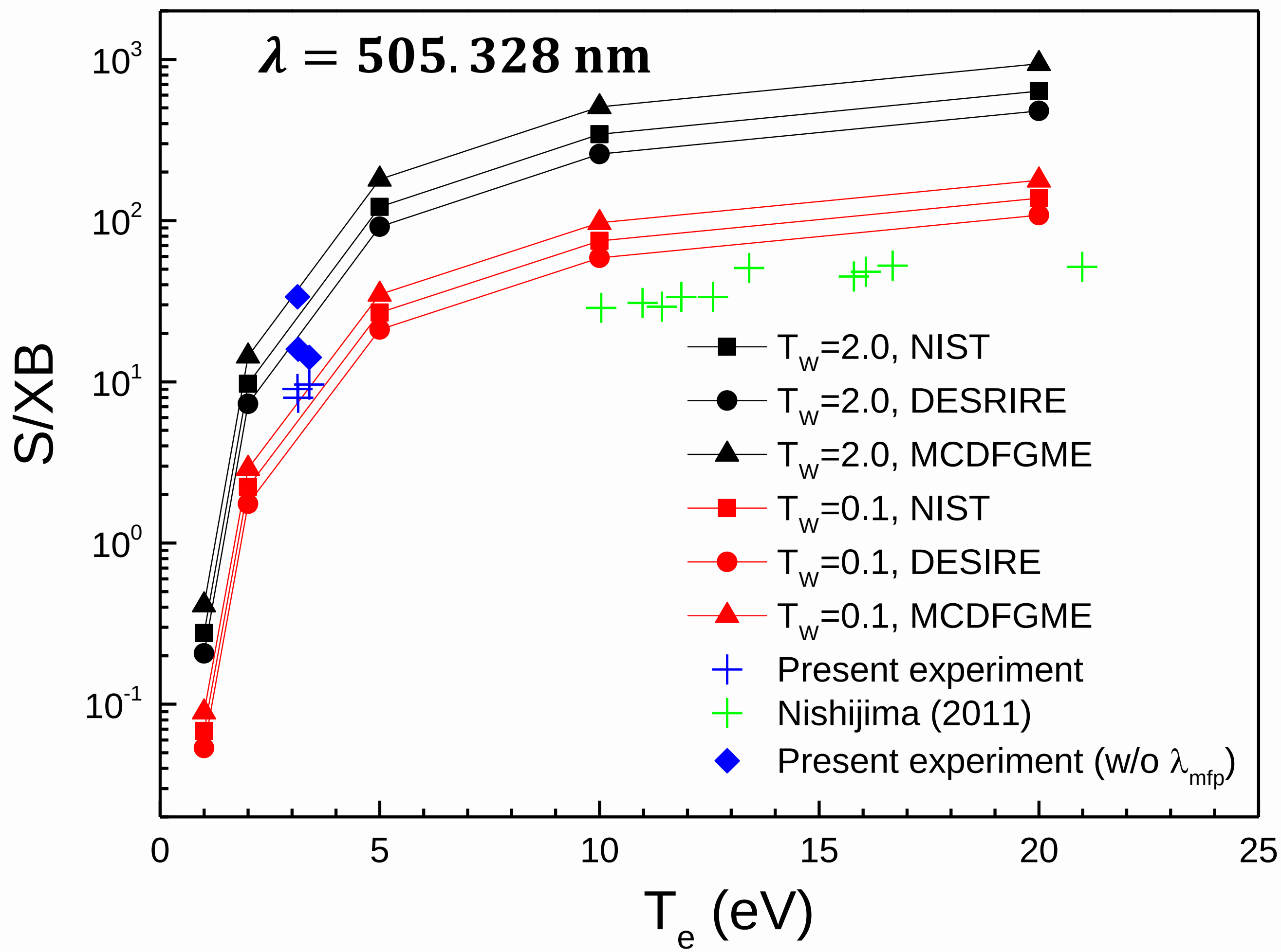

D. Nishijima et al., Phys. Plasmas **18** 019901 (2011), Erratum of Phys. Plasmas **16** 122503 (2009)

S/XB by EIE cross section from DARC calculation and a CRM

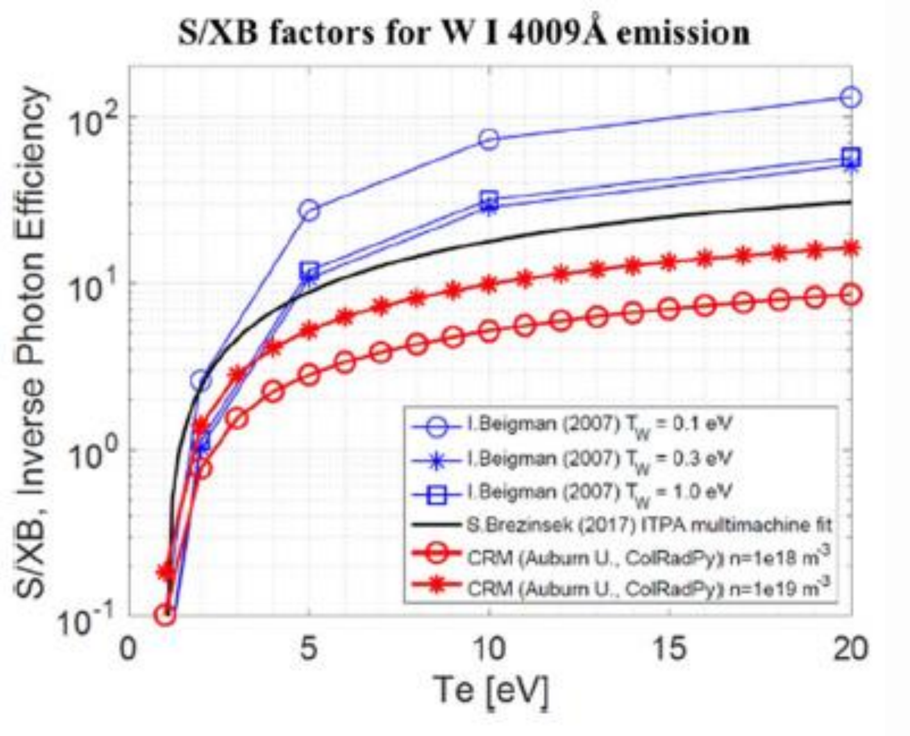

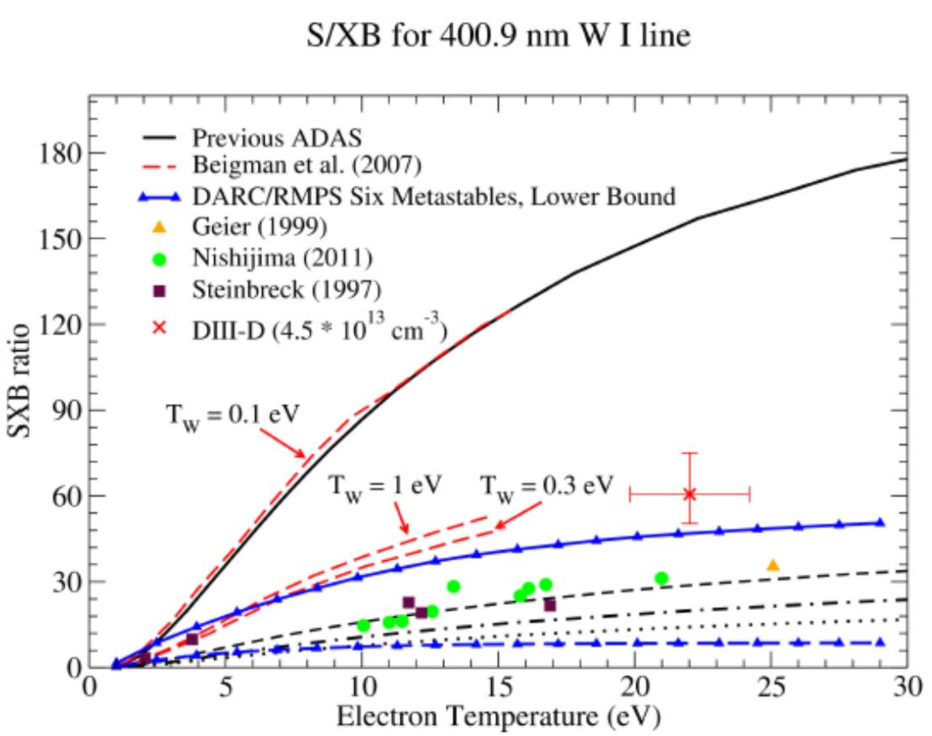

C. C. Kepler et al., Plasma Phys. Control. Fusion **64** 104008 (2022)

C. J. Favreau, Ph. D thesis, Auburn Univ. (2019)

Further effects to be considered

Opacity, Optical trapping

$$\frac{S}{XB} = \frac{\eta\Gamma_{\mathrm{W}^+}}{4\pi I_{\mathrm{WI}}} = \frac{\eta Y\Gamma_i}{4\pi I_{\mathrm{WI}}} \times \left\{1 - \exp\left(-\frac{L}{\lambda_{mfp}}\right)\right\}, \ \eta < 1.0$$

Optical cascade from upper levels

Finally, more accurate collisional-radiative modeling considering other processes such as diffusion etc.

Other models for EII(E) cross sections

Binary Encounter Bethe (BEB) model for EII

(Y.-K. Kim and M. E. Rudd, Phys. Tev. A **50** 3954 1994)

$$\sigma_{\mathrm{neut}} = \frac{4\pi a_0^2 N R^2}{B^2[t + (u+1)/m]}\left[\frac{\ln t}{2}\left(1 - \frac{1}{t^2}\right) + 1 - \frac{1}{t} - \frac{\ln t}{t+1}\right]$$

N : The orbital occupation number
B : The orbital binding energy,
t = T/B for incident electron energy T
u = U/B for the orbital kinetic energy U
Constant m = 1 for K- and L-shell, m=n of other orbitals

BE scaled plane wave Born (PWB) cross section for EIE

(Y.-K. Kim, Phys. Rev. A **64** 032713 2001)

$$\sigma_{\mathrm{BE}} = \frac{T}{T + B + E}\sigma_{\mathrm{PWB}}$$

E : The excitation energy

Summary and outlook

- Collisional-radiative modeling (CRM) for He, H/D plasma

✓ The CRM solves nonlinear steady state balance equations including processes such as radiation trapping and heavy particle collisions self-consistently for low temperature regime. Sensitivities of line spectra and particle densities to used AM data and plasma parameters are investigated.

✓ Charge exchanges such as $\mathrm{H}^+ + \mathrm{H}_2 \rightarrow \mathrm{H} + \mathrm{H}_2^+$ etc. will be considered in the CRM for H.

✓ CRM for H taking into account for molecular vibrational states will be performed.

Summary and outlook

- S/XB ratio for sputtering yield of W

✓ S/XB ratios for W I were spectroscopically measured in KPBIF and compared with model calculations using EII/EIE and radiative transition data.

✓ New atomic data by metastable resolved BEB cross section for EII and BE scaled PWB cross section for EIE combined with MCDF calculation will be used for the S/XB calculation.

Our group members

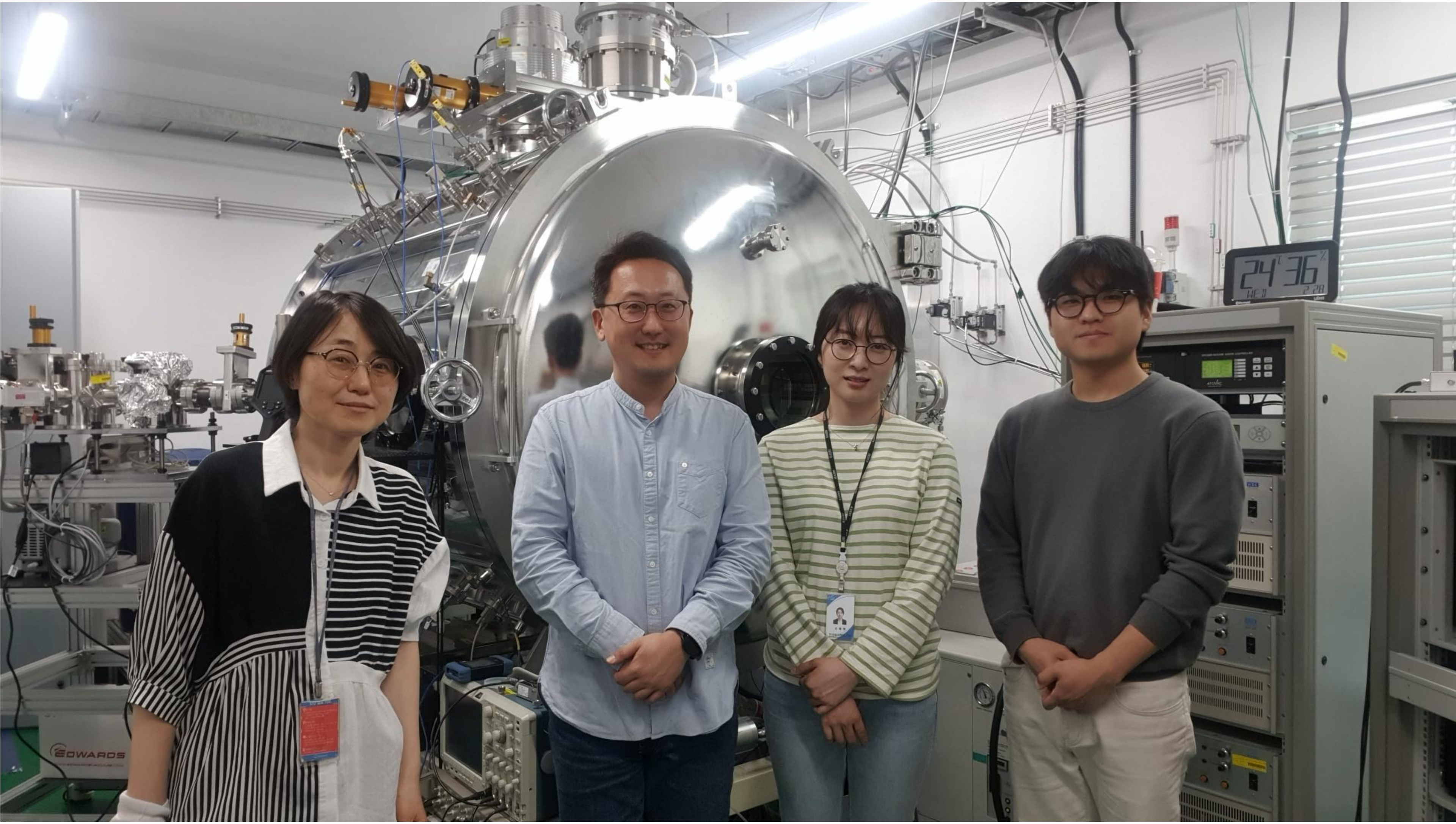

Acknowledgements

- **Wonho Choe**, Gas discharge physics lab., Korea Advanced Institute of Science and Technology, Daejeon, Rep. of Korea
- **Octavio Roncero**, Quantum molecular dynamics, Instituto de Física Fundamental, Madrid, Spain
- **Dmitry Fursa**, MCCC molecular data, Curtin Institute for Computation and Department of Physics, Astronomy and Medical Radiation Sciences, Curtin University, Australia